NASA Technical Paper 1631

A Theoretical Analysis of Simulated Transonic Boundary Layers in Cryogenic-Nitrogen Wind Tunnels

Jerry B. Adcock and Charles B. Johnson

MARCH 1980

NASA

NASA Technical Paper 1631

A Theoretical Analysis of Simulated Transonic Boundary Layers in Cryogenic-Nitrogen Wind Tunnels

Jerry B. Adcock and Charles B. Johnson
Langley Research Center
Hampton, Virginia

National Aeronautics
and Space Administration

**Scientific and Technical
Information Office**

1980

SUMMARY

A theoretical analysis has been made to determine the real-gas effects on simulation of transonic boundary layers in wind tunnels with cryogenic nitrogen as the test gas. Transonic Mach numbers and the stagnation pressures and temperatures anticipated for such tunnels were considered in the analysis. The analysis includes calculated results for laminar and turbulent flat-plate boundary layers as well as turbulent boundary layers on a two-dimensional airfoil. The results indicate that the adiabatic cryogenic-nitrogen boundary layers are not substantially different from ideal-gas boundary layers, with the maximum difference of the various boundary-layer parameters being on the order of 1 percent. At the maximum tunnel pressure (9.0 atm), the real-gas deviations of the boundary-layer parameters were opposite in sign from those at 1.0 atm and were of the same order of magnitude. The analysis shows this result was produced by opposite effects with a relative dominance that is a function of pressure. One of these effects is due to a change in the slope of the viscosity-temperature curve and the other is due to the combined effects of thermal and caloric imperfections as well as the changing of the other transport properties.

Nonadiabatic boundary layers are adequately simulated if the wall enthalpy ratio is reproduced rather than the temperature ratio. Adiabatic wall temperatures and static temperature profiles are found to be considerably different for cryogenic nitrogen. However, since none of the other profiles or integrated boundary-layer parameters are appreciably different, there seems to be no significant consequence to this difference. For turbulent boundary layers on an airfoil, the boundary-layer parameters for cryogenic nitrogen deviate most from an ideal gas in the strongly favorable pressure gradient near the leading edge. However, the deviations are not of sufficient magnitude to produce concern about simulating boundary layers in the presence of either favorable or adverse pressure gradients.

INTRODUCTION

Transonic wind tunnels that use pressurized cryogenic nitrogen as the test gas are being designed and built in this country (ref. 1) and in Europe (ref. 2) in order to obtain a higher test Reynolds number capability. The Reynolds number capability, generally increased by operating at increased pressure as well as at reduced temperature, should provide better simulation of full-scale transonic-flight aerodynamics. However, if appreciable real-gas effects on flow simulation are encountered in the high-pressure cryogenic environment, then either correction procedures will have to be developed or certain limitations on the test conditions will be required, with a corresponding reduction in Reynolds number capability.

Various studies have examined the real-gas effects of cryogenic nitrogen on inviscid flows and found them to be insignificant (refs. 3 to 6). With

regard to viscous flows, Wagner and Schmidt have performed a very limited real-gas analysis of laminar boundary-layer–shock-wave interactions (ref. 7). Care should be exercised when assessing the magnitudes of real-gas effects from the tunnel conditions that were analyzed, however, because the one set of conditions that produced large real-gas effects was at a stagnation pressure (p_t = 39.0 atm) much greater than is practical for transonic wind tunnels.

This paper presents the results of a theoretical real-gas analysis that assesses the magnitude of real-gas effects on the simulation of transonic-flight boundary layers due to testing in pressurized cryogenic-nitrogen wind tunnels. Specifically, this study covers the stagnation pressure range (1.0 to 9.0 atm) and the stagnation-temperature range (300 K down to liquefaction) of the National Transonic Facility (ref. 1). The scope of this study includes numerical analysis of both laminar and turbulent boundary layers on a flat plate and turbulent boundary layers on a two-dimensional airfoil.

SYMBOLS

C_f	local skin-friction coefficient
c	airfoil chord
c_p	specific heat at constant pressure
H	enthalpy
k	eddy thermal conductivity
M	Mach number
p	pressure, atm (1 atm = 101.3 kPa)
N_{Pr}	turbulent Prandtl number, $c_p\varepsilon/k$
R	Reynolds number
T	temperature, K
u	tangential velocity
x	streamwise distance from leading edge of plate or airfoil
y	normal distance from plate surface
α	angle of attack, deg
δ	boundary-layer thickness (u/u_∞ = 0.995)
δ^*	boundary-layer displacement thickness
ε	eddy viscosity

ϑ boundary-layer momentum thickness

μ absolute viscosity, N-s/m^2

ρ density

Subscripts:

aw adiabatic wall value

t stagnation value

w wall value

X value based on a length of X

∞ free-stream value

APPROACH

Air at the temperatures and pressures of transonic flight has the characteristics of an ideal (i.e., thermally and calorically perfect) diatomic gas. Therefore, for this analysis, analytical results for the real-gas boundary-layer solutions at the cryogenic-tunnel conditions are compared with results for an ideal diatomic gas (nitrogen at standard conditions, i.e., 1.0 atm and 300 K) at the same Mach number and Reynolds number. This approach is consistent with the assumption that transonic-flight boundary layers would be perfectly simulated in a very large nitrogen tunnel operating at standard conditions. This should be the case since both nitrogen and air at standard conditions have the thermodynamic characteristics of an ideal diatomic gas and have essentially the same transport properties.

In this analysis, two real-gas boundary-layer computer programs were used in the computations. The first of these is a laminar boundary-layer similar-solution program based on the procedure of Cohen (ref. 8). The second program solves equations for laminar or turbulent boundary-layer flows of ideal gases or reacting-gas mixtures in chemical equilibrium and is applicable to two-dimensional and axisymmetric configurations (refs. 9 and 10). Both of these programs use thermodynamic and transport property tables. For the present analysis, these tables for cryogenic nitrogen are based on the equations of reference 11.

For the Anderson and Lewis program (ref. 9), the fully implicit option was employed. For turbulent boundary layers, the Reichardt eddy viscosity law was used for the inner region of the layer and instantaneous transition was assumed at the leading edge. The Sutherland viscosity law was used for ideal-gas solutions. A constant value of 0.9 was used for the turbulent Prandtl number N_{Pr} in both ideal- and real-gas solutions. For other options such as grid spacing and convergence criteria, the values recommended in reference 10 were used.

RESULTS AND DISCUSSION

The computer programs previously discussed have been used to obtain real-gas boundary-layer solutions for various types of boundary layers. These include laminar and turbulent flat-plate boundary layers at adiabatic and nonadiabatic conditions and adiabatic turbulent boundary layers on a two-dimensional airfoil. These solutions were made for a tunnel stagnation-pressure range of 1.0 to 9.0 atm and a tunnel stagnation-temperature range of liquefaction to 300 K. The corresponding ideal-nitrogen-gas solutions were also obtained at standard conditions and at the same Mach number and Reynolds number so that the real-gas effects on the boundary-layer simulation could be determined.

Laminar Flat-Plate Boundary Layers

The real-gas effects of cryogenic nitrogen on the simulation of laminar flat-plate (zero pressure gradient) boundary layers were analyzed first since both programs calculate this type of boundary layer very accurately and the results provided a check on the correctness of the interfacing of nitrogen-property tables with the programs. For analysis purposes, a stagnation pressure of 9.0 atm and a stagnation temperature of 120 K were chosen because it was believed that the largest real-gas effects would occur at the extreme operating conditions, which are near the nitrogen saturation boundary and approximate the maximum Reynolds number condition of the National Transonic Facility (ref. 1). The free-stream Mach number was set at 0.85. (For this Mach number and pressure, the stagnation temperature which produces free-stream saturation is 110 K.) Solutions were obtained for the zero-heat-transfer case and for various heat-transfer conditions (T_w/T_t from 0.87 to 2.50).

The boundary-layer parameters resulting from the solutions are presented in figure 1. These results show that the laminar boundary-layer parameters as predicted by the two real-gas programs are in excellent agreement with regard to both trends and magnitudes. After this finding, the Anderson and Lewis program was used exclusively in the analysis because of its greater versatility.

As shown in figure 1, these results indicate only small differences between the real- and ideal-gas boundary-layer parameters at adiabatic conditions. The following table gives the ratio of the real-gas nitrogen values (from Anderson and Lewis program) to the ideal-gas values at adiabatic conditions:

Parameter	Nitrogen/Ideal
C_f	0.992
θ	.993
δ^*	1.000
δ	.999

The adiabatic wall temperature ratio T_{aw}/T_t is measurably lower (about 2.5 percent) for cryogenic nitrogen than for the ideal gas. However, the adiabatic wall enthalpy ratio for cryogenic nitrogen ($H_{aw}/H_t = 0.989$) differs from the ideal value (0.981) by less than 1 percent. Hence, at nonadiabatic conditions for which appreciable real-gas effects are indicated, the enthalpy ratio may provide a better correlating parameter than the temperature ratio. This possibility is verified by the results presented in figure 2. Thus, for the nonadiabatic tunnel experiments, the ratio of wall enthalpy to total enthalpy should be used to simulate transonic-flight ratios of wall temperature to total temperature ($H_w/H_t = T_w/T_t$).

The real-gas effects of cryogenic nitrogen on the adiabatic laminar boundary-layer profiles for conditions of 9.0 atm and 120 K are illustrated in figure 3 in which the nitrogen profiles are presented relative to the ideal-gas profiles. The calculated velocity profiles are so nearly identical for the real and ideal cases that their ratio does not differ from a value of 1.0 at the scale of this plot. Except for the static temperature, the profiles are very similar, with the maximum difference at any point being 1 percent or less. The cryogenic-nitrogen temperature ratios remain less than the ideal values throughout the boundary layer. This difference is thought to be primarily associated with the cryogenic-nitrogen enthalpies being functions of both temperature and pressure while the ideal-gas enthalpy is only a function of temperature ($H = c_pT$). The static-enthalpy profiles differ by only 0.5 percent or less. At any rate, there do not seem to be any important consequences of the temperature profiles being different since the integrated boundary-layer parameters θ and δ^* and skin friction are not appreciably affected by this difference.

It should be noted that the boundary layer is not likely to remain laminar to this Reynolds number; but the magnitudes of real-gas effects were essentially the same at any longitudinal plate location (Reynolds number).

Most cryogenic-tunnel testing will be done at adiabatic boundary-layer conditions. Thus, a study was made of the effect of the various tunnel test variables on adiabatic laminar boundary-layer simulation. First, boundary-layer solutions were calculated for a Mach number of 0.95 for the range of stagnation temperatures (300 K down to near liquefaction) at stagnation pressures of 1.0 and 9.0 atm. These solutions are presented in relative form in figures 4 to 7. At 1.0 atm, the nitrogen boundary-layer parameters are generally higher than the ideal-gas values (less than 1.0 percent) with the deviation initially increasing with decreased temperature. However, at about 120 K, the deviations begin to decrease and continue to go down as the liquefaction boundary is approached. This reversal in trend was unexpected. It had been anticipated that the real-gas effects would be largest at the minimum temperature since the deviation of the thermodynamic properties from the ideal values continually increase with decreasing temperature. Another surprising result is that at 9.0 atm the trends in the deviations are not similar to the trends at 1.0 atm and, at the lowest temperatures, are opposite to the deviations at 1.0 atm (i.e., the nitrogen values are less than the ideal values). This latter effect is more obvious in figure 8, in which solutions obtained at a constant temperature of 120 K and various stagnation pressures are presented. At 1.0 atm, all of the nitrogen boundary-layer parameters are greater than the

corresponding ideal values. As stagnation pressure is increased, the relative values decrease almost linearly, with all values at 9.0 atm being less than 1.0. This kind of variation of real-gas effects with pressure would indicate that there are compensating real-gas effects taking place. Evidence that this is the case will be presented in the section on turbulent boundary layers.

Boundary-layer solutions were also made to determine the effect of Mach number on the magnitude of real-gas effects. The solutions were obtained at a pressure of 9.0 atm and at a temperature (150 K) high enough to avoid liquefaction at a Mach number of 2.0. The results are presented in relative form in figure 9 for Mach numbers from 0.4 to 2.0. For this range, only the deviation of displacement thickness is a strong function of Mach number, with the maximum deviation of 1.3 percent at Mach 2.0.

The real-gas effects on laminar boundary layers due to testing in cryogenic nitrogen that have been presented are well within the boundary-layer measuring accuracies. These effects are not large enough to produce concern about the simulation of flat-plate laminar boundary layers in a cryogenic-nitrogen tunnel.

Turbulent Flat-Plate Boundary Layers

A similar analytical investigation of the real-gas effects on a turbulent boundary layer was also conducted. The results of these calculations are presented in figures 10 to 18. These results are very similar to those for the laminar boundary layers and indicate that for the operating range of the cryogenic-nitrogen tunnel, real-gas effects on the simulation of flat-plate turbulent boundary layers will be negligible.

Wagner and Schmidt, in their work on laminar boundary-layer—shock-wave interactions (ref. 7), noted the role played by counteracting real-gas effects. That is, an effect due to a change in the slope of the viscosity-temperature curve was being opposed by the combined effects of all other real-gas characteristics. As can be seen from the viscosity curves for nitrogen (fig. 19), the slope at cryogenic temperatures is somewhat steeper than at ambient temperatures. To verify the findings of Wagner and Schmidt, two different kinds of solutions for the real-gas boundary layers were calculated by using two different approaches. First, real-gas solutions were calculated with the viscosity table changed so that the slope of the viscosity-temperature curve was constant and equal to the slope at ambient temperature and pressure. These solutions should show the combined real-gas effects with the viscosity-slope change removed. In the second approach, ideal-gas solutions were calculated as usual, except that viscosity slopes representative of cryogenic-nitrogen values were used. These solutions should show the effects of the change in viscosity slope only. These two types of solutions and the usual real-gas solution relative to the normal ideal-gas solution are presented in figure 20. Here again the solutions were made at various pressures for T_t = 120 K and M_∞ = 0.85. The parameter presented is local skin friction. The real-gas effects with constant viscosity slope are such that the skin-friction values are lower than those for the ideal gas. This deviation increases with increasing pressure, as one might anticipate from viewing the thermodynamic-property deviations from ideal-gas behavior. The effect of the changing viscosity slope with the ideal-gas solu-

tions is such that the skin-friction values are higher than those for the ideal-gas case. Because the viscosity slope for cryogenic nitrogen decreases with increasing pressure (fig. 19) and actually becomes closer to the slope at ambient temperature, this effect decreases with increased pressure. Notice that these two effects can be summed to give a fairly good representation of the total real-gas effects. Also note that these two effects are about the same order of magnitude, with the viscosity-slope effect being slightly dominant at 1.0 atm and the other real-gas effects being dominant at 9.0 atm. This agrees with the trends that Wagner and Schmidt (ref. 7) have suggested and explains the real-gas deviations with tunnel pressure and temperature. Fortunately, these combined real-gas deviations are small and do not affect the simulation of turbulent flat-plate boundary layers in cryogenic-nitrogen tunnels.

Turbulent Boundary Layers on a Two-Dimensional Airfoil

Turbulent boundary-layer solutions for a two-dimensional airfoil were calculated in order to determine the effect of pressure gradients on the magnitudes of real-gas effects. The Anderson and Lewis program (ref. 9) does not include any interaction of the external flow with the boundary layer except through the pressures that are impressed on the boundary layer. The flow properties at the edge of the boundary layer were calculated by assuming isentropic expansion of the gas from stagnation conditions to the local pressure. For the ideal-gas solutions, these are straightforward calculations, but for real-gas solutions an isentropic expansion table for each set of stagnation conditions must be provided before the start of the boundary-layer calculations for that particular set of conditions.

The airfoil pressure distribution (fig. 21) that was chosen for the analysis is that for the NACA 0012-64 airfoil at zero angle of attack and at $M_\infty = 0.85$ (ref. 12). There is a strongly favorable pressure gradient near the leading edge and a nearly constant favorable gradient from the 10-percent-chord position to the 60-percent-chord position. A shock produces a strongly adverse gradient at the 60-percent-chord position and milder adverse gradients continue to the trailing edge.

Boundary-layer solutions were calculated at various stagnation temperatures and a pressure of 1.0 atm. These solutions relative to ideal-gas solutions are shown in figures 22 to 24. In the slightly favorable pressure-gradient region (10 to 60 percent of the chord), the real-gas deviations with temperature are very similar to those for the flat plate (figs. 13 to 15). In the strongly favorable pressure-gradient region near the leading edge, the relative values of all the boundary-layer parameters become larger as the leading edge is approached. Forward of the 1- to 2-percent-chord stations, the relative values are uncertain due to the numerics of the program and are greatly influenced by such things as the number of input pressures, the smoothness of the pressure curve, the interval of the isentropic expansion table, and the boundary-layer starting procedure. Nevertheless, this trend of an increasing real-gas effect in favorable pressure gradients has been confirmed by calculations made for the boundary layer on the front face of a cylinder. For the cylinder the favorable gradient existed over a much longer length and the deviations could be more easily extrapolated to the leading edge. The maximum

deviations for the cylinder were on the order of 1 percent. For the forward region of the airfoil, the relative values of the boundary-layer parameters are reflections of the pressure distribution (fig. 21), with the largest deviations occurring at the regions of the highest pressures or pressure gradients. This must be a real-gas effect associated with the pressure-gradient effect on nonsimilar boundary layers rather than an effect associated with the magnitude of pressure because these deviations are opposite to the flat-plate deviations as functions of pressure (fig. 17).

In the adverse pressure-gradient region at the shock, the relative values of the boundary-layer parameters (except for C_f) are again reflections of the pressure distribution as described above. For this section of the airfoil, as well as for the rest of the airfoil, the real-gas deviations are small and insignificant.

Boundary-layer solutions were finally calculated for various stagnation pressures and a stagnation temperature of 120 K. These solutions relative to the ideal-gas solutions are shown in figures 25 to 27 and indicate that the real-gas effects associated with the magnitude of pressure are opposite to those that are associated with pressure gradients, as indicated previously. Also note from these results that the magnitudes of real-gas effects at the highest pressure (9.0 atm) are of the same order as those at 1.0 atm and are insignificant.

CONCLUSIONS

A real-gas analysis of boundary-layer simulation in cryogenic-nitrogen, pressurized transonic wind tunnels has been made. The analysis resulted in the following conclusions:

1. Generally, the deviations of the cryogenic-nitrogen boundary-layer parameters from the corresponding ideal-gas values are on the order of 1 percent or less and are thought to be insignificant in terms of adequately simulating boundary layers in such a tunnel.

2. Nonadiabatic flat-plate boundary layers (both laminar and turbulent) can be properly simulated in the cryogenic-nitrogen tunnels if the tunnel enthalpy ratio H_w/H_t is the correlating parameter rather than the temperature ratio T_w/T_t.

3. Adiabatic wall temperature ratios T_{aw}/T_t for cryogenic-nitrogen boundary layers are measurably different from those of the ideal gas at ambient temperature. Differences exist in the static temperature profiles corresponding to this wall temperature difference. However, since the other adiabatic boundary-layer profiles (velocity, density, and enthalpy) and other important boundary-layer parameters (θ, δ^*, and C_f) are not appreciably different for cryogenic nitrogen, there does not seem to be a significant consequence of the difference in the static temperature profiles.

4. As indicated in the work of Wagner and Schmidt (ref. 7), the magnitudes of real-gas effects due to testing in cryogenic nitrogen can be understood by

considering two counteracting effects. One is due to operating on a different viscosity-temperature slope. The other is a combination of all other real-gas characteristics which include thermal and caloric imperfections as well as changes in the other transport-property characteristics. These two effects are opposing and the present study indicates that they produce only minor real-gas deviations in the various boundary-layer parameters. The relative dominance of these two effects causes the real-gas deviations of cryogenic nitrogen at 9.0-atm pressure to be opposite to those at 1.0 atm and about the same order of magnitude.

5. Studies of turbulent boundary layers on a two-dimensional airfoil show the largest real-gas effects occurring in the strongly favorable pressure gradient near the leading edge of the airfoil. None of the differences encountered are large enough to prevent adequate simulation of boundary layers in the presence of either favorable or adverse pressure gradients.

Langley Research Center
National Aeronautics and Space Administration
Hampton, VA 23665
January 28, 1980

REFERENCES

1. Howell, Robert R.; and McKinney, Linwood W.: The U.S. 2.5-Meter Cryogenic High Reynolds Number Tunnel. High Reynolds Number Research, Donald D. Baals, ed., NASA CP-2009, 1977, pp. 27-51.

2. Christophe, Jean: Genèse du Projet de Soufflerie Transsonique Européene à Grand Nombre de Reynolds (Genesis of the Project of European High Reynolds Number Transonic Wind Tunnel). L'Aéronautique et L'Astonautique, no. 72, 1978, pp. 21-34.

3. Adcock, Jerry B.: Real-Gas Effects Associated With One-Dimensional Transonic Flow of Cryogenic Nitrogen. NASA TN D-8274, 1976.

4. Adcock, Jerry B.; Kilgore, Robert A.; and Ray, Edward J.: Cryogenic Nitrogen as a Transonic Wind Tunnel Test Gas. AIAA Paper 75-143, Jan. 1975.

5. Albone, C. M.: An Investigation Into the Real Gas Effects of Cryogenic Nitrogen in Inviscid Homentropic Flow. First International Symposium on Cryogenic Wind Tunnels, Dep. Aeronaut. & Astronaut., Univ. of Southampton, Apr. 1979, pp. 17.1-17.4.

6. Wagner, Bernhard; and Schmidt, Wolfgang: Theoretical Investigations of Real Gas Effects in Cryogenic Wind Tunnels. AIAA J., vol. 16, no. 6, June 1978, pp. 580-586.

7. Wagner, Bernhard; and Schmidt, Wolfgang: Theoretical Investigations of Real Gas Effects in Cryogenic Wind Tunnels. AIAA Paper 77-669, June 1977.

8. Cohen, Nathaniel B.: Boundary-Layer Similar Solutions and Correlation Equations for Laminar Heat-Transfer Distribution in Equilibrium Air at Velocities up to 41,000 Feet Per Second. NASA TR R-118, 1961.

9. Anderson, E. C.; and Lewis, C. H.: Laminar or Turbulent Boundary-Layer Flows of Perfect Gases or Reacting Gas Mixtures in Chemical Equilibrium. NASA CR-1893, 1971.

10. Miner, E. W.; Anderson, E. C.; and Lewis, Clark H.: A Computer Program for Two-Dimensional and Axisymmetric Nonreacting Perfect Gas and Equilibrium Chemically Reacting Laminar, Transitional and/or Turbulent Boundary Layer Flows. VPI-E-71-8, May 1971. (Available as NASA CR-132601.)

11. Jacobsen, R. T.; Stewart, R. B.; McCarty, R. D.; and Hanley, H. J. M.: Thermophysical Properties of Nitrogen From the Fusion Line to 3500 R (1944 K) for Pressures to 150 000 psia (10 342 × 10^5 N/m^2), NBS Tech. Note 648, U.S. Dep. Com., Dec. 1973.

12. Hall, Robert M.: Onset of Condensation Effects With an NACA 0012-64 Airfoil Tested in the Langley 0.3 Meter Transonic Cryogenic Tunnel. NASA TP-1385, 1979.

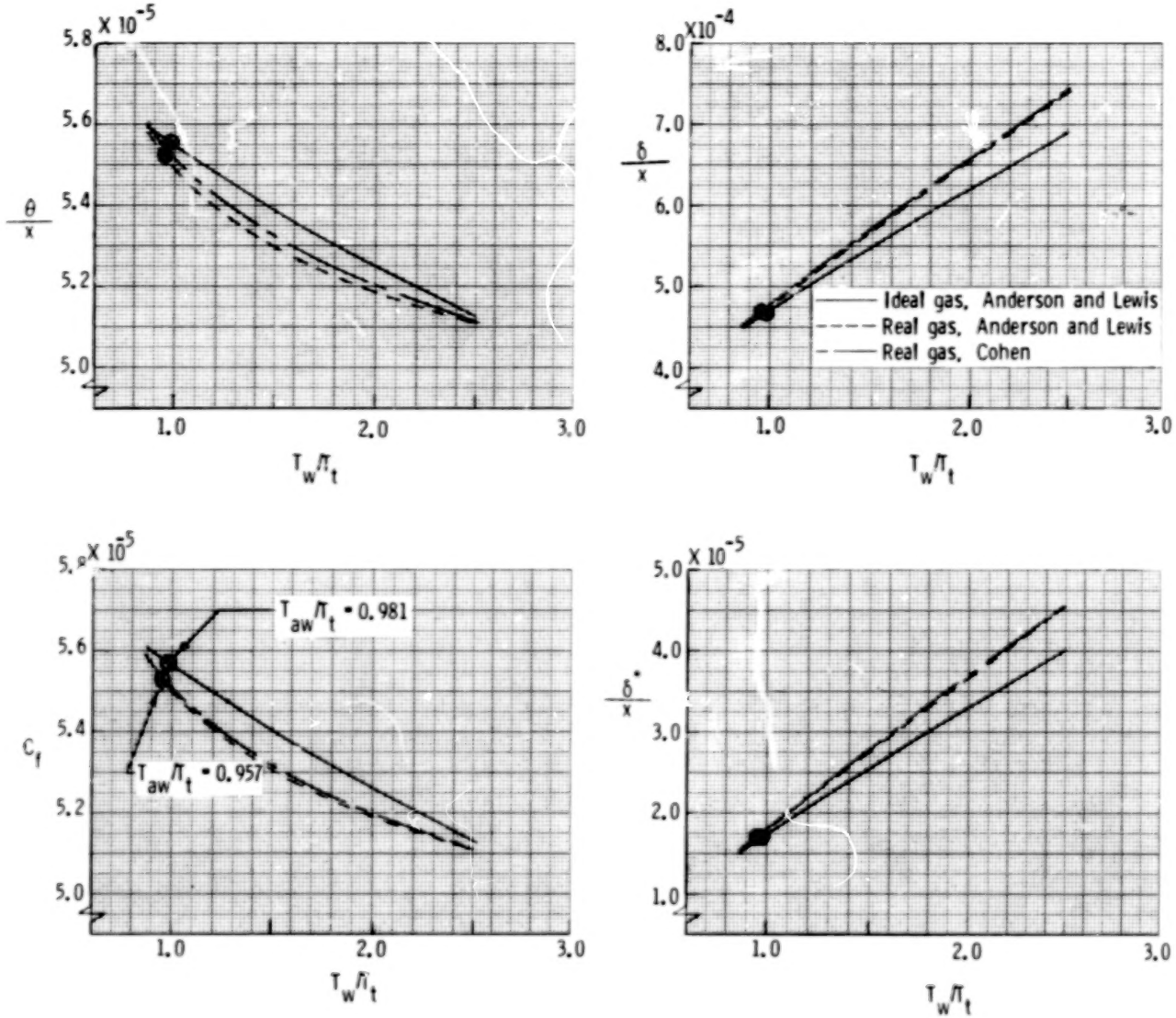

Figure 1.- Real-gas effects of cryogenic nitrogen on laminar boundary-layer parameters for a flat plate at various wall temperature conditions. $M_\infty = 0.85$; $p_t = 9.0$ atm; $T_t = 120$ K; $R_X = 140 \times 10^6$.

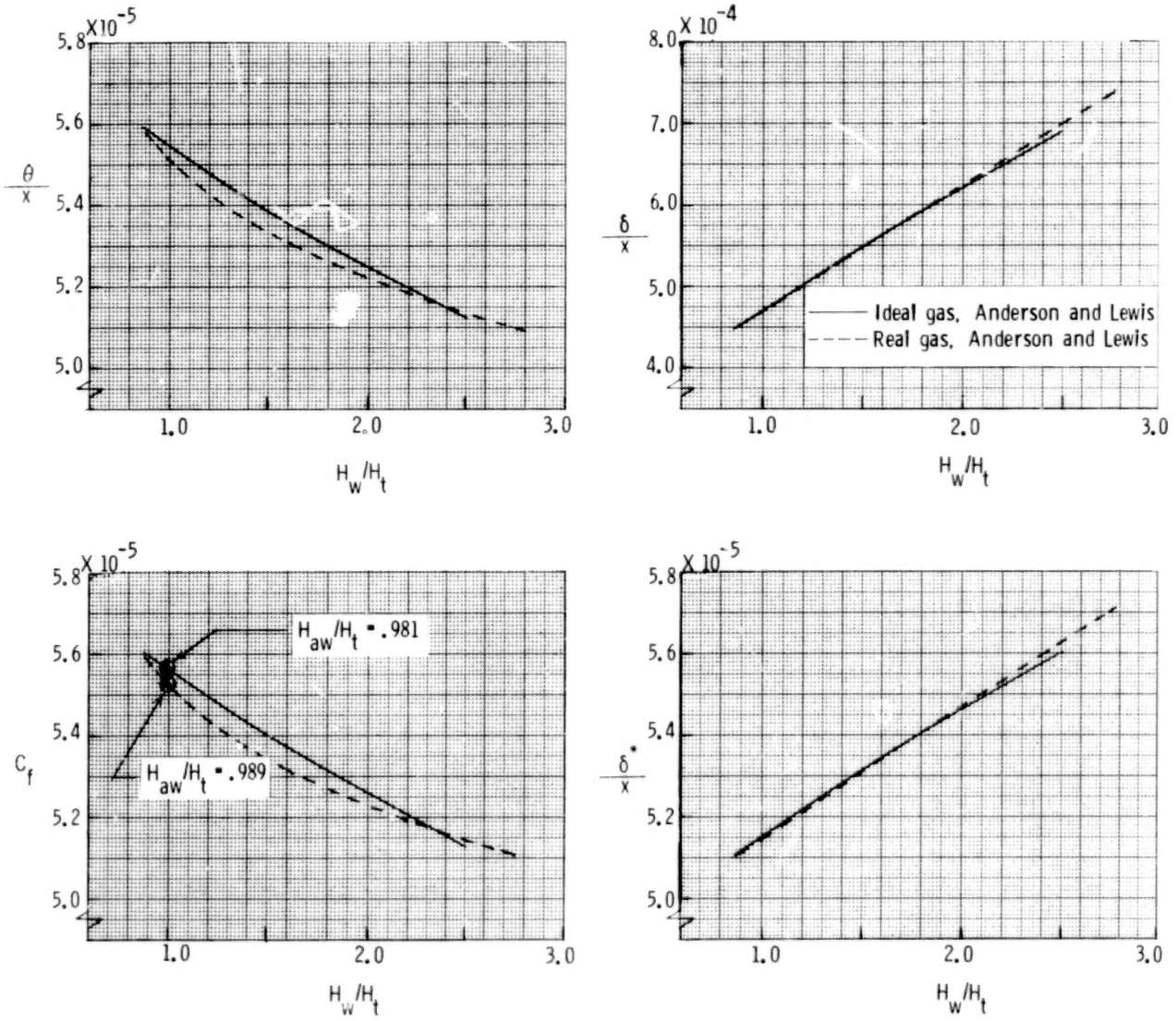

Figure 2.- Real-gas effects of cryogenic nitrogen on laminar boundary-layer parameters for a flat plate at various wall enthalpy conditions. $M_\infty = 0.85$; $p_t = 9.0$ atm; $T_t = 120$ K; $R_X = 140 \times 10^6$.

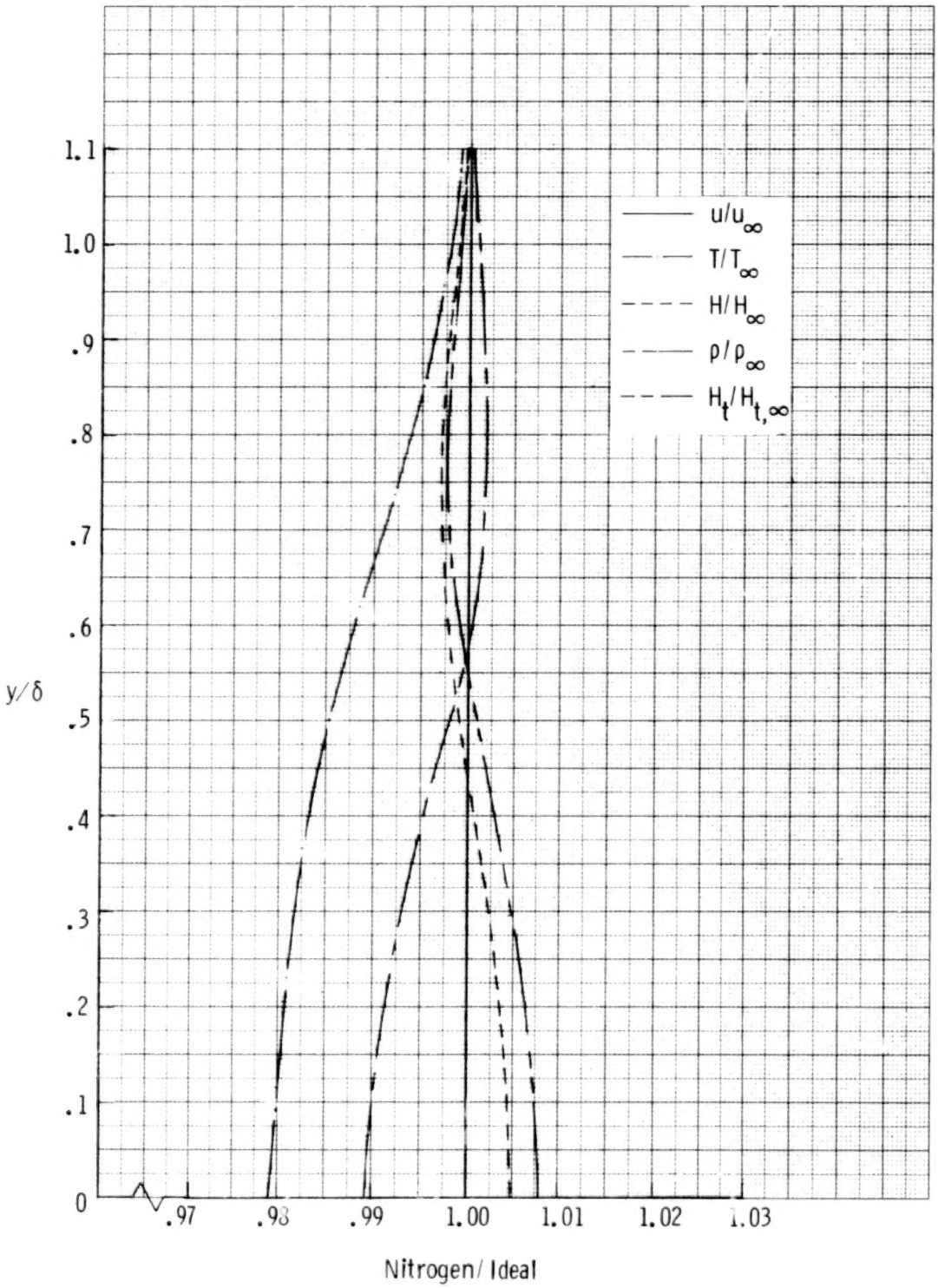

Figure 3.- Relative laminar adiabatic profiles for a flat plate. $M_\infty = 0.85$; $p_t = 9.0$ atm; $T_t = 120$ K; $R_X = 140 \times 10^6$.

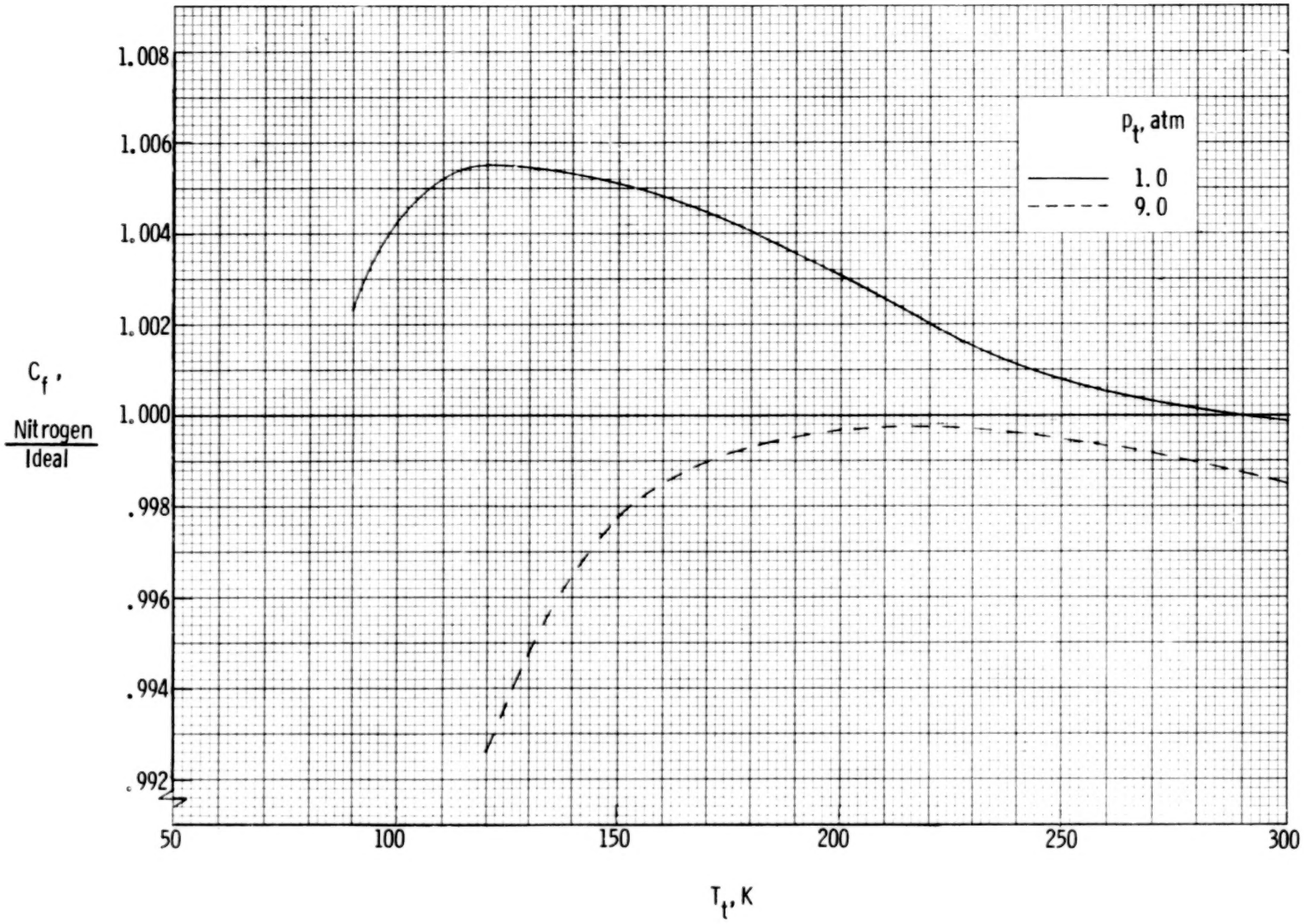

Figure 4.- Relative local skin-friction coefficients for adiabatic laminar boundary layers on a flat plate at various tunnel stagnation temperatures. $M_\infty = 0.85$.

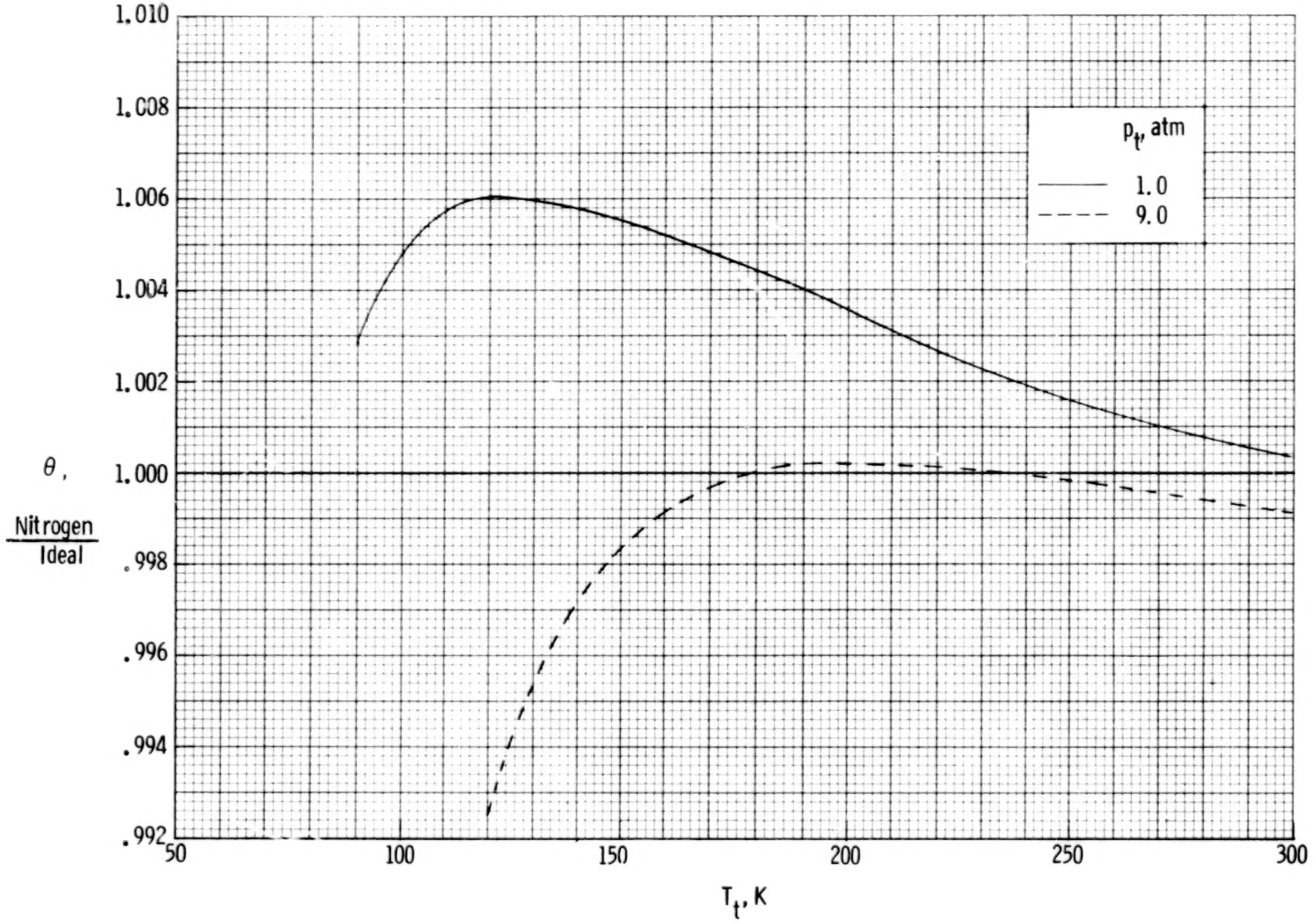

Figure 5.- Relative momentum thicknesses for adiabatic laminar boundary layers on a flat plate at various tunnel stagnation temperatures. $M_\infty = 0.85$.

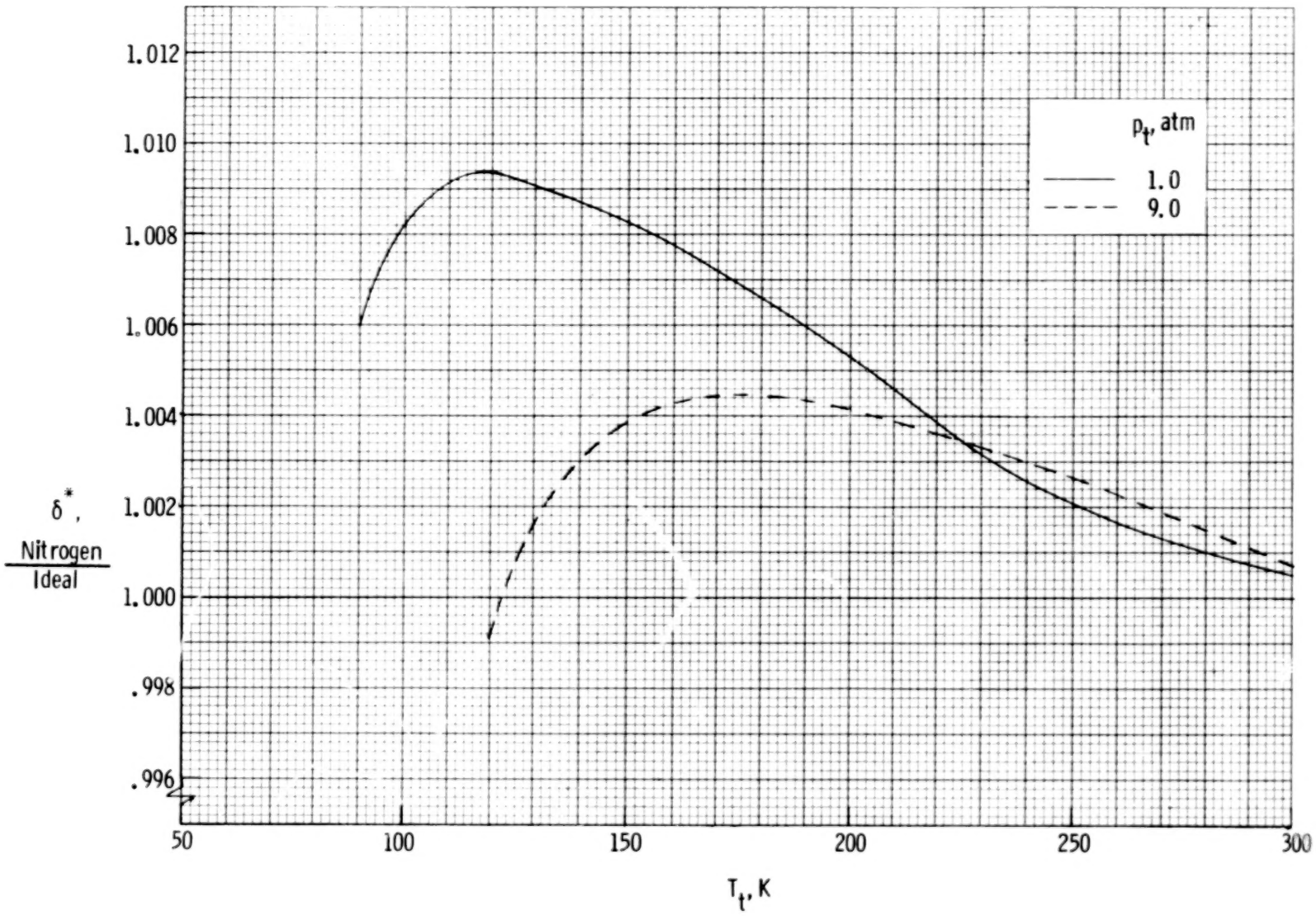

Figure 6.- Relative displacement thicknesses for adiabatic laminar boundary layers on a flat plate at various tunnel stagnation temperatures. $M_\infty = 0.85$.

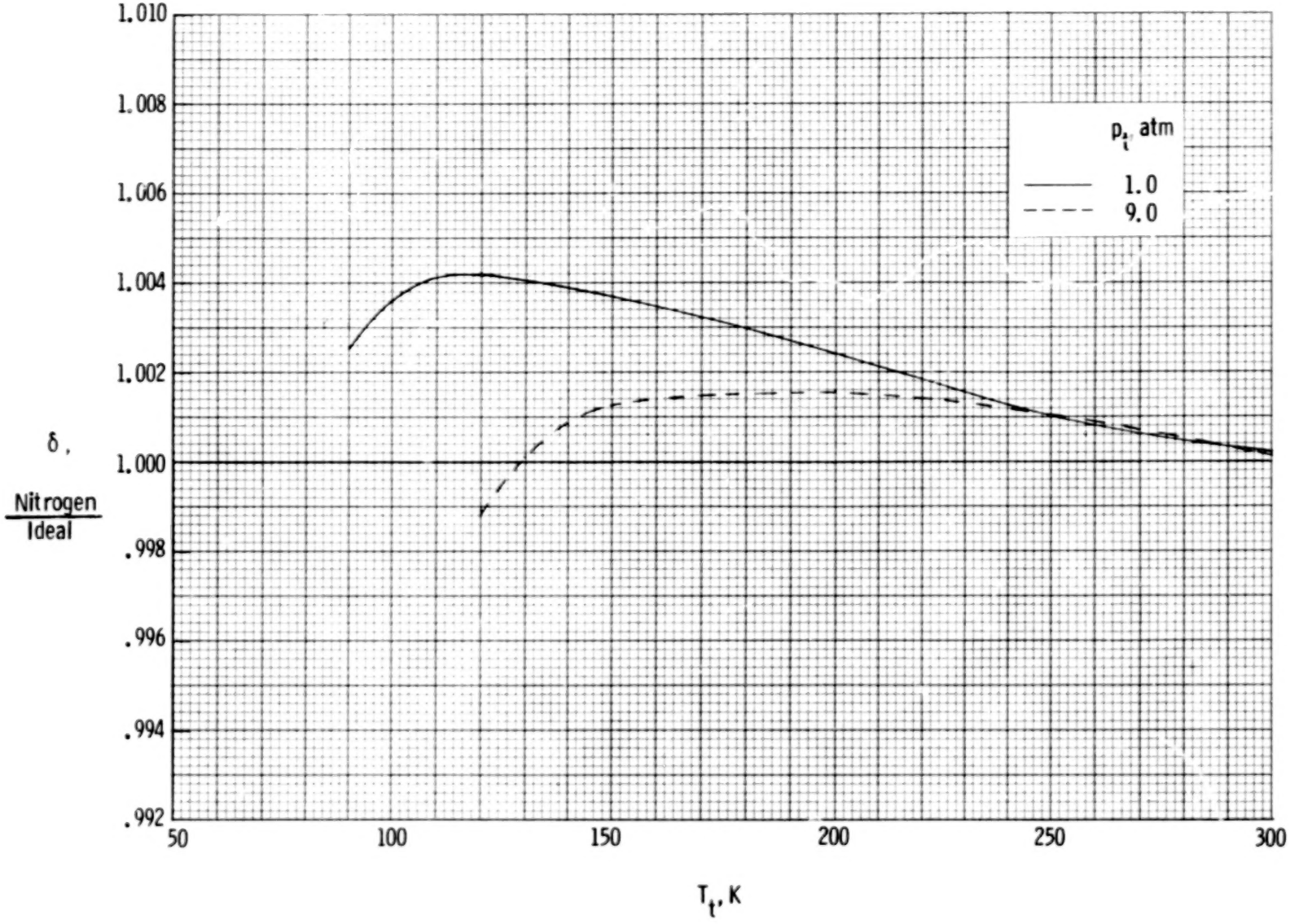

Figure 7.- Relative thicknesses for adiabatic laminar boundary layers on a flat plate at various tunnel stagnation temperatures. $M_\infty = 0.85$.

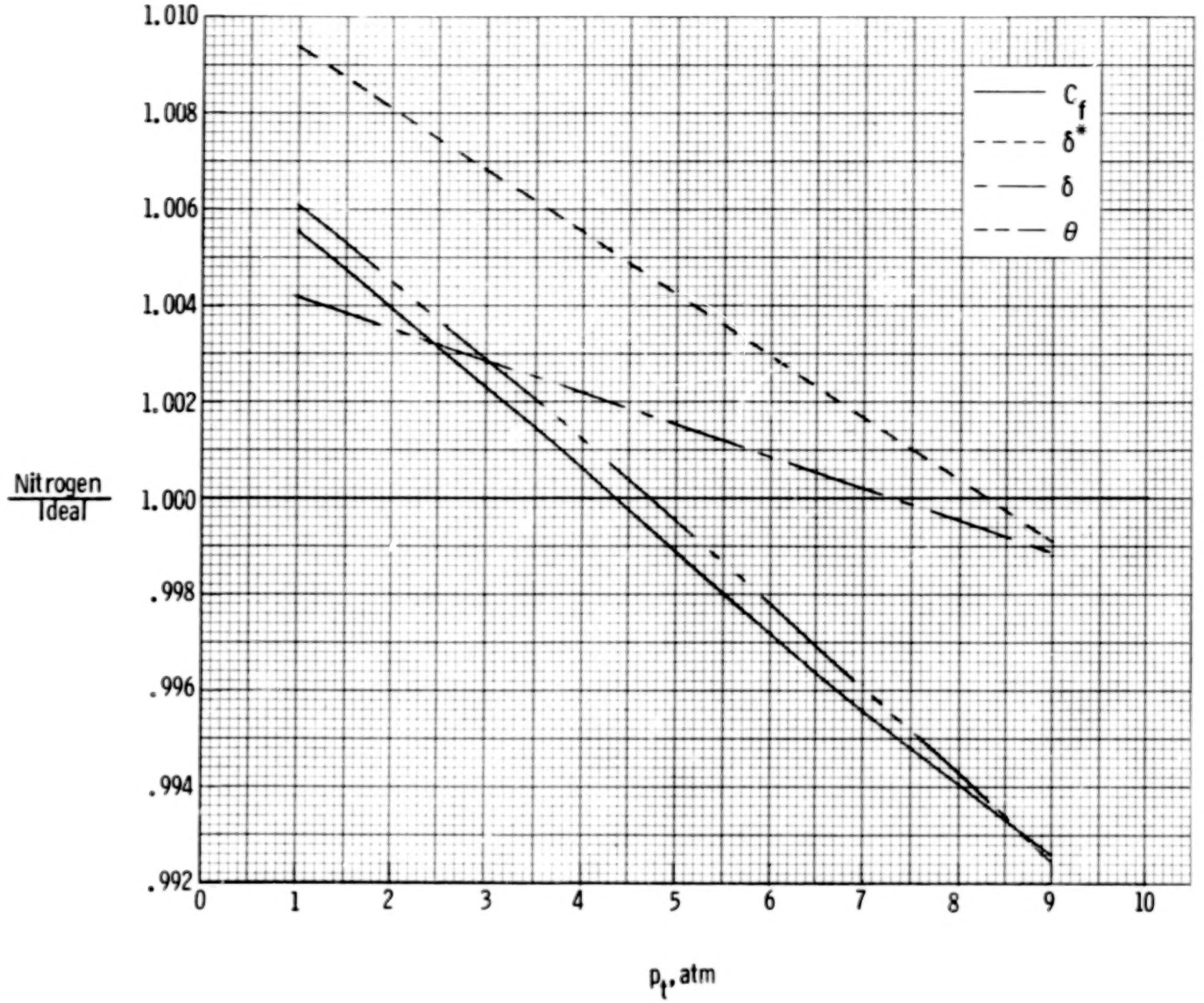

Figure 8.- Relative values for parameters for adiabatic laminar boundary layers on a flat plate at various tunnel stagnation pressures. $M_\infty = 0.85$; $T_t = 120$ K.

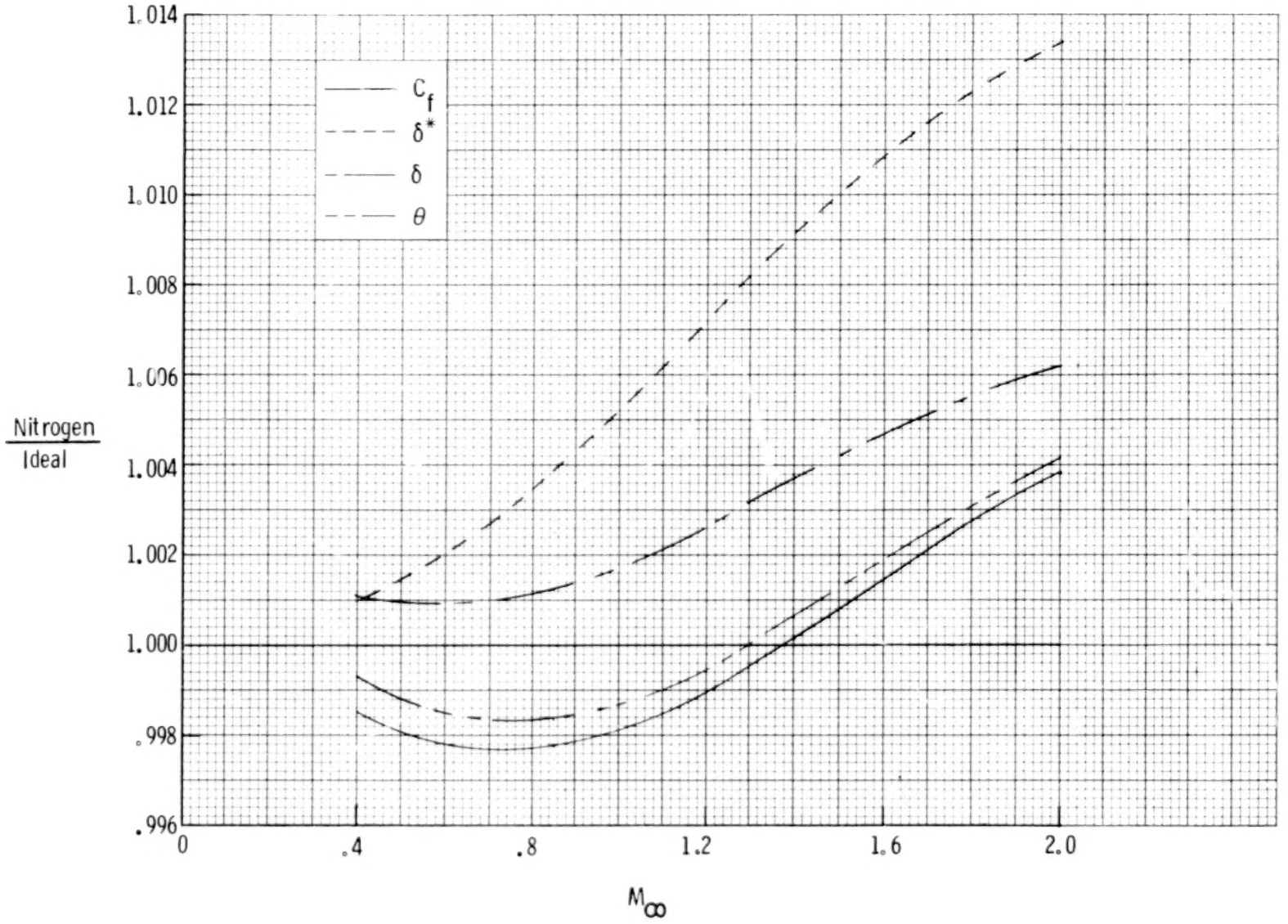

Figure 9.- Relative values for parameters for adiabatic laminar boundary layers on a flat plate at various free-stream Mach numbers. p_t = 9.0 atm; T_t = 150 K.

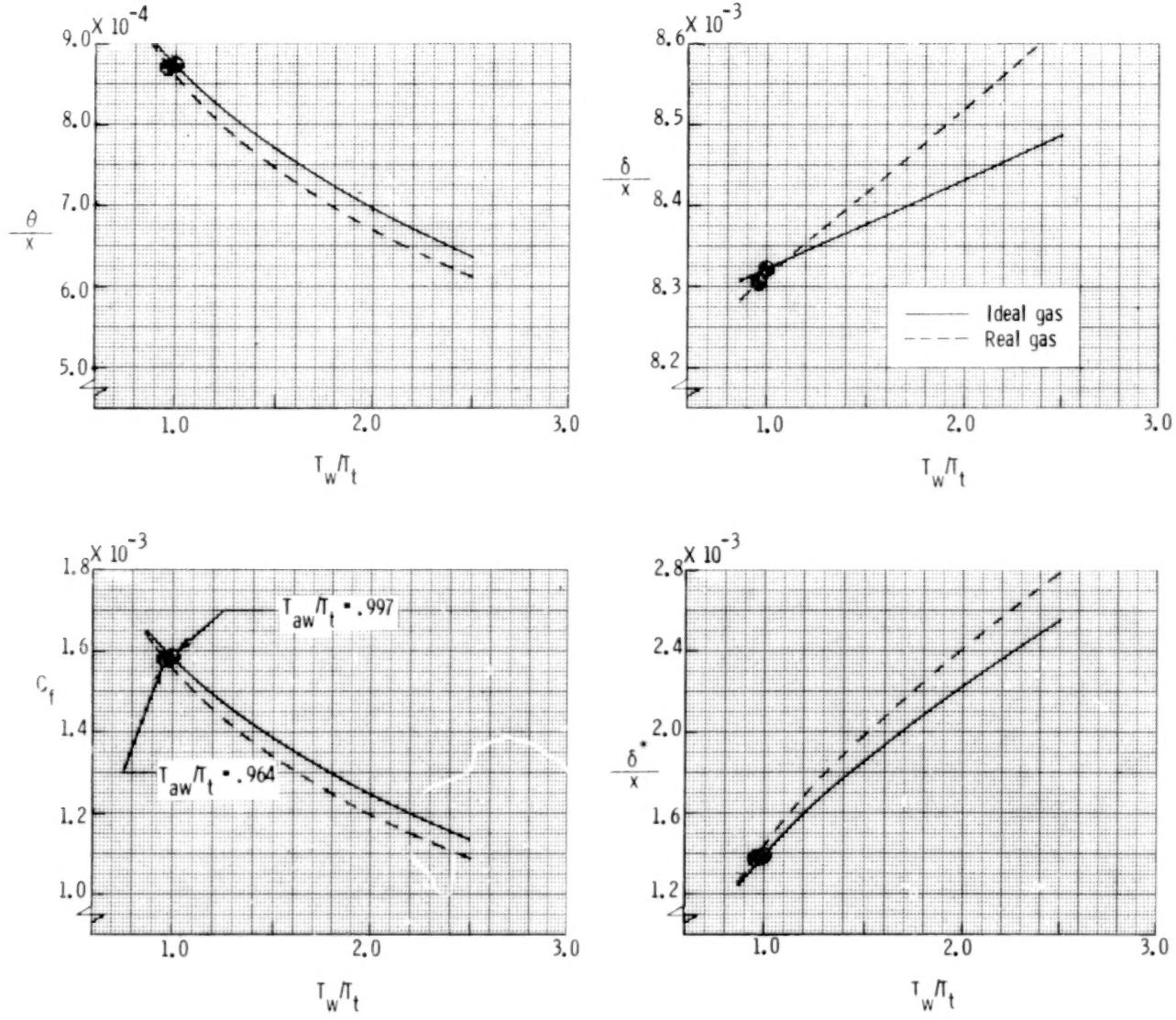

Figure 10.- Real-gas effects of cryogenic nitrogen on turbulent boundary-layer parameters for a flat plate at various wall temperature conditions. M_∞ = 0.85; p_t = 9.0 atm; T_t = 120 K; R_X = 140 × 10^6.

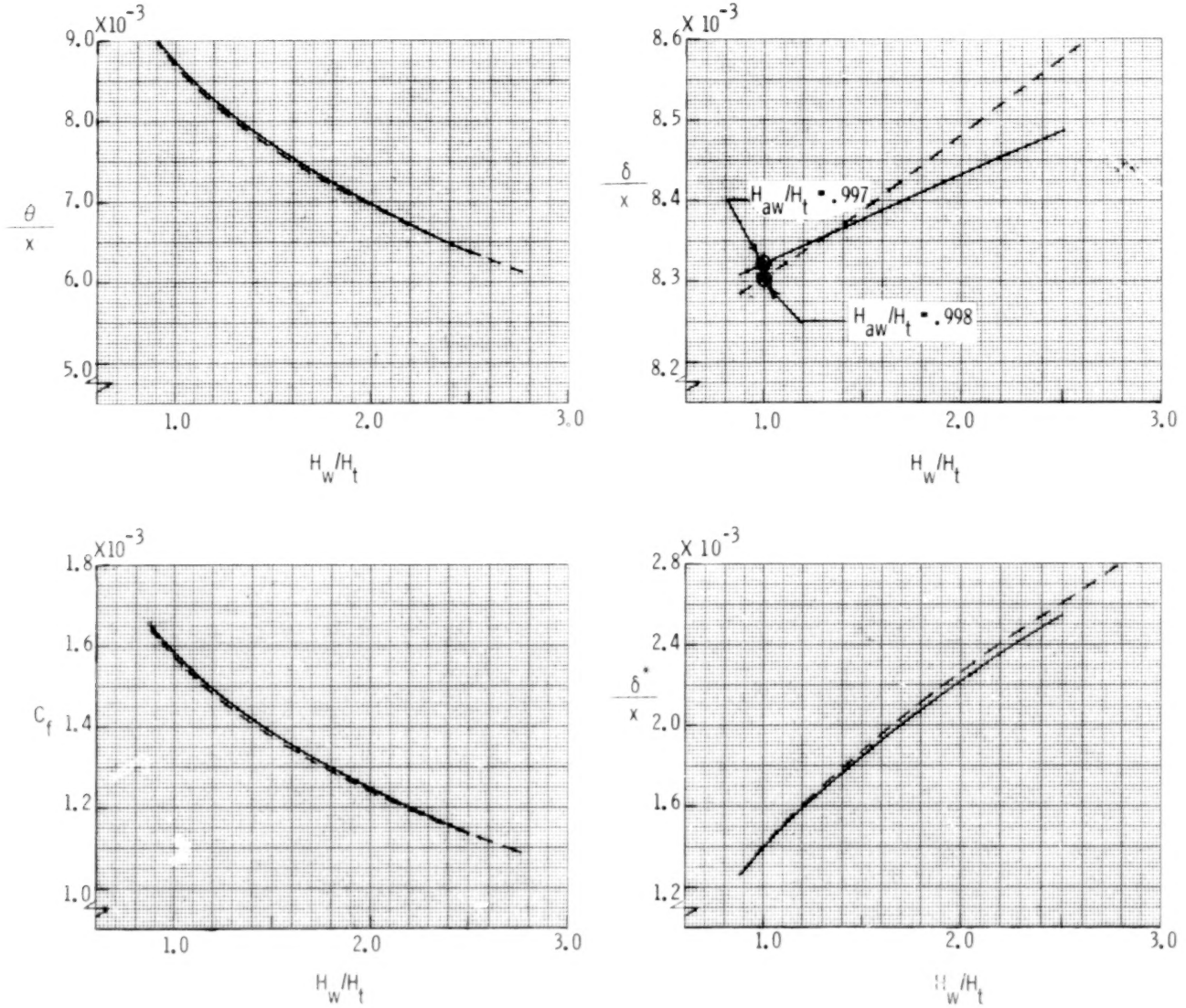

Figure 11.- Real-gas effects of cryogenic nitrogen on turbulent boundary-layer parameters for a flat plate at various wall enthalpy conditions. $M_\infty = 0.85$; $p_t = 9.0$ atm; $T_t = 120$ K; $R_X = 140 \times 10^6$.

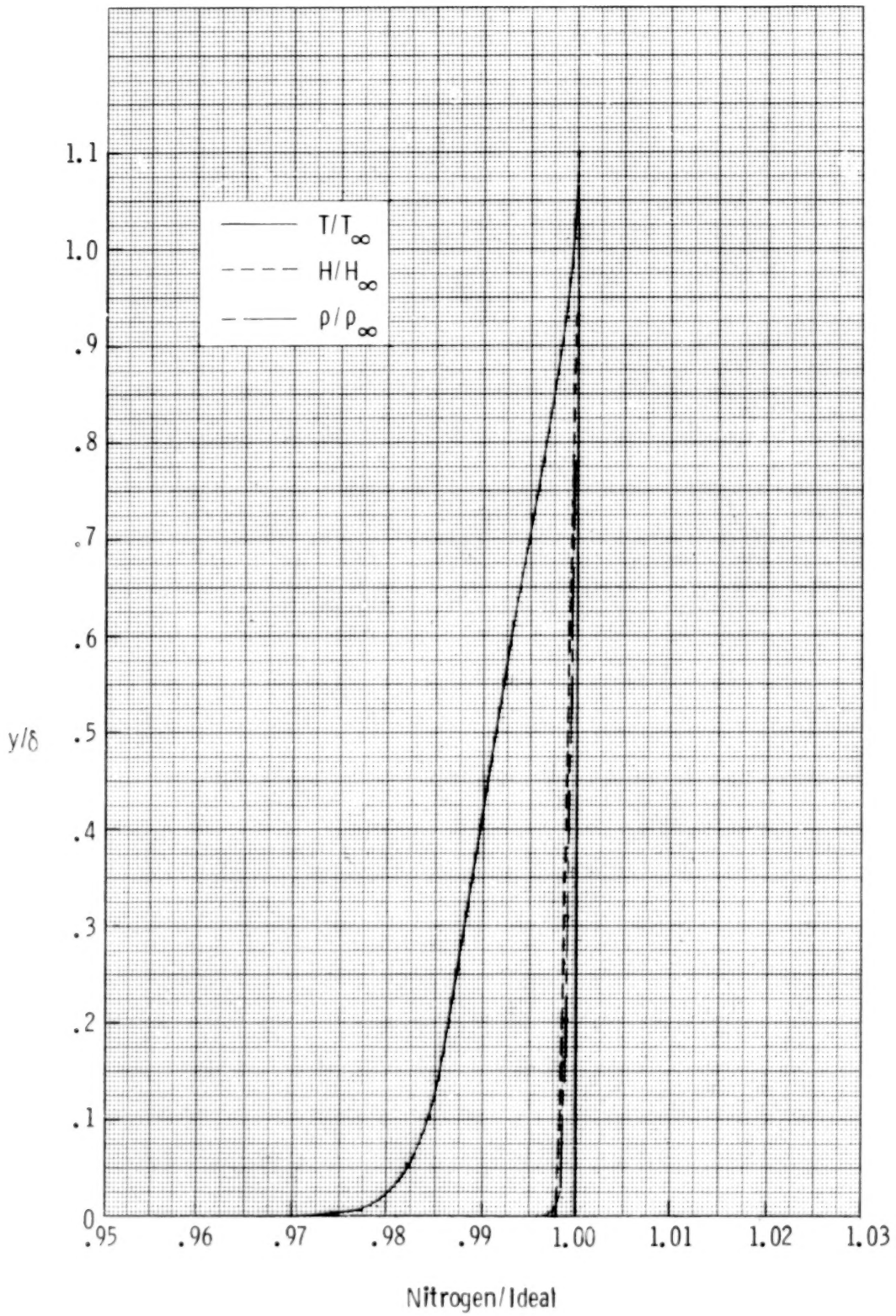

Figure 12.- Relative turbulent adiabatic profiles for a flat plate. $M_\infty = 0.85$; $p_t = 9.0$ atm; $T_t = 120$ K; $R_X = 140 \times 10^6$.

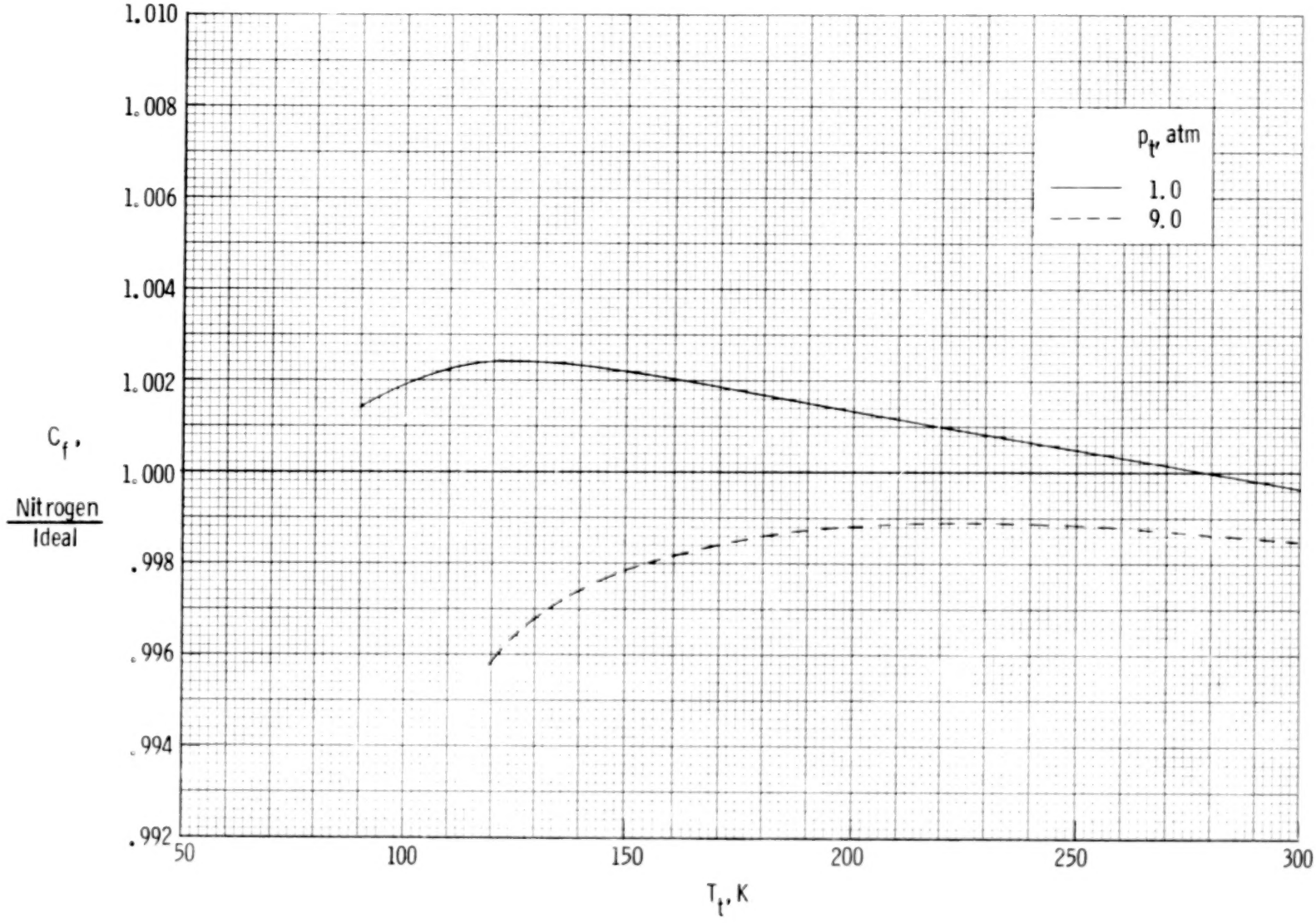

Figure 13.- Relative local skin-friction coefficients for adiabatic turbulent boundary layers on a flat plate at various tunnel stagnation temperatures. $M_\infty = 0.85$.

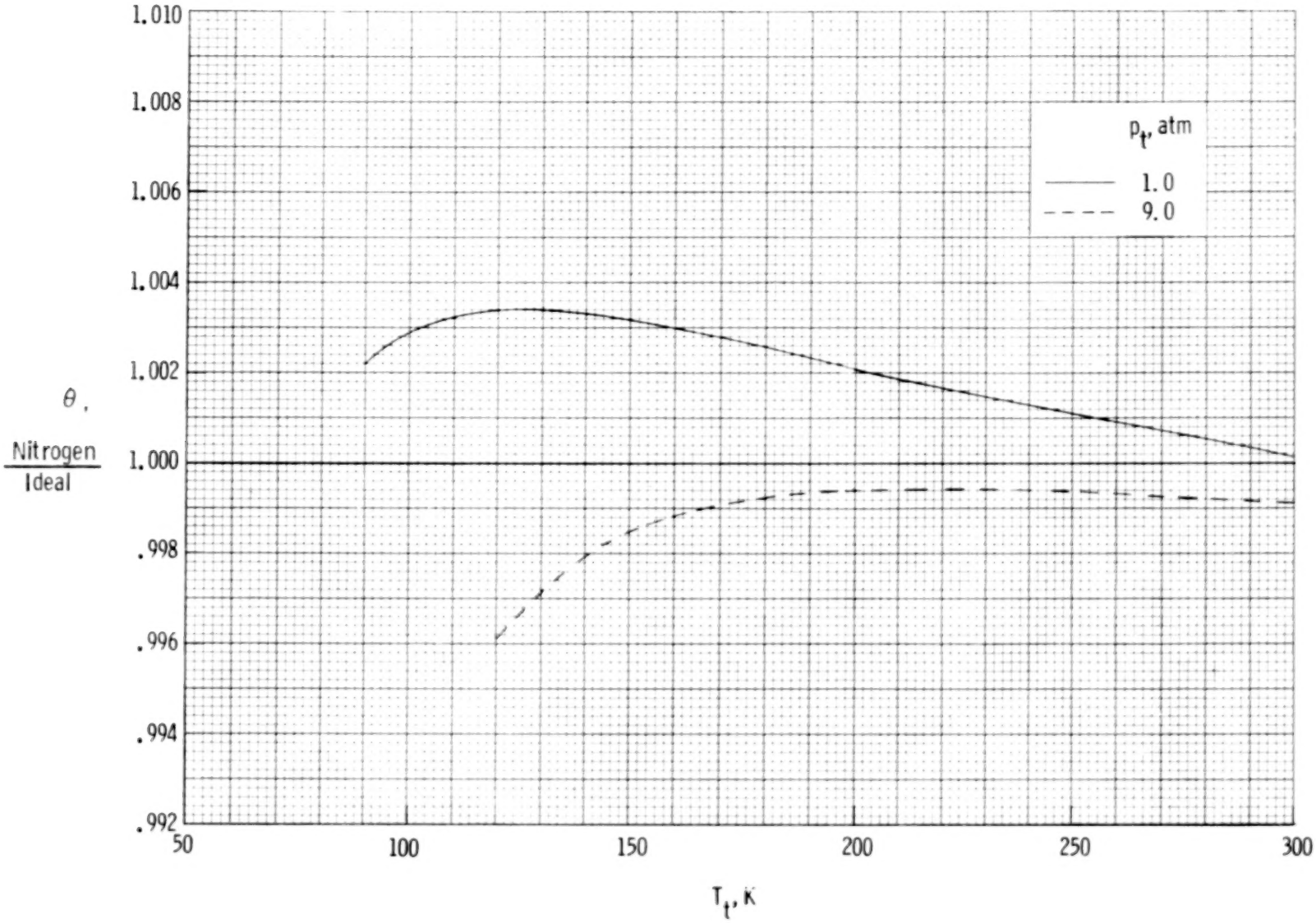

Figure 14.- Relative momentum thicknesses for adiabatic turbulent boundary layers on a flat plate at various tunnel stagnation temperatures. $M_\infty = 0.85$.

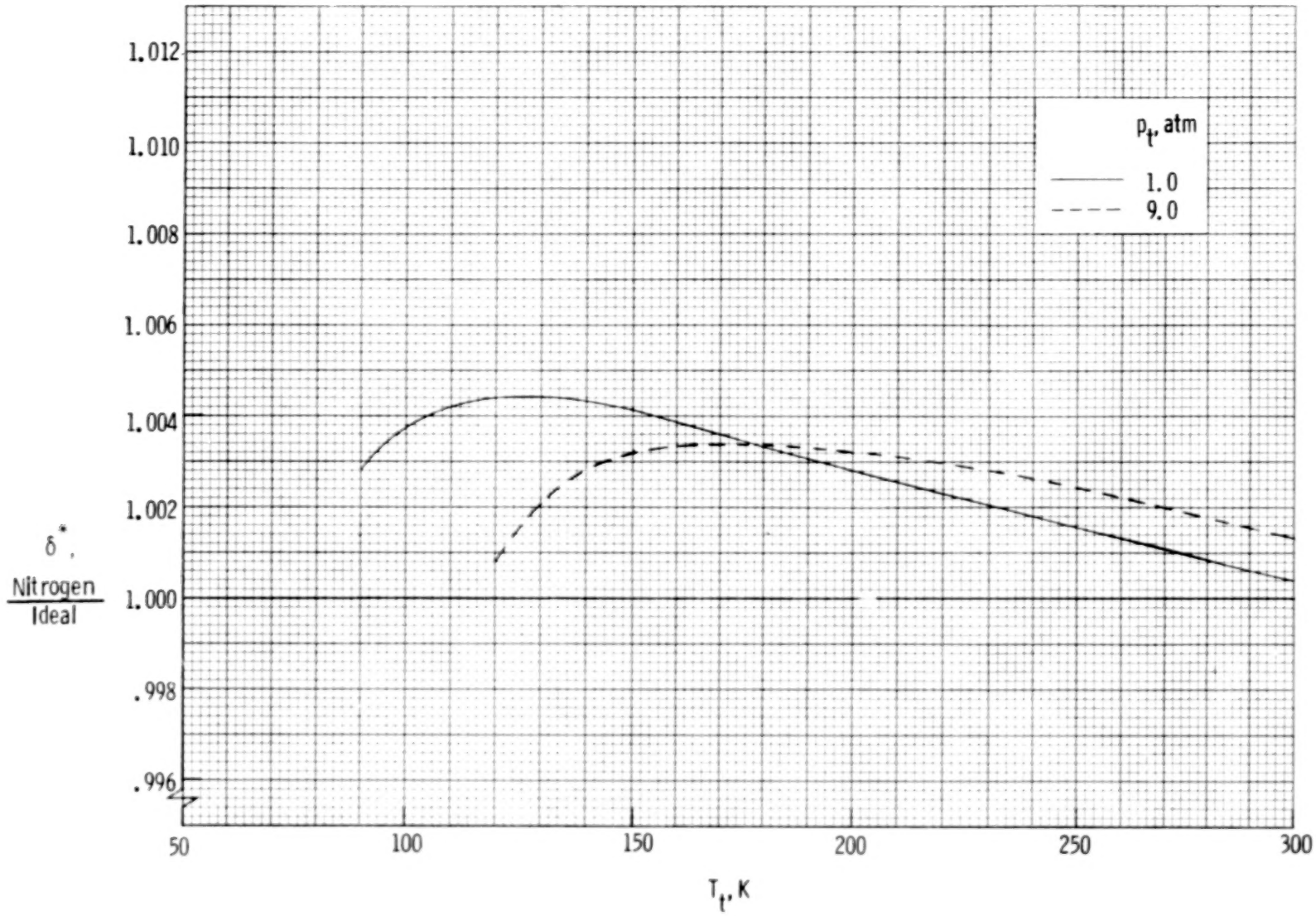

Figure 15.- Relative displacement thicknesses for adiabatic turbulent boundary layers on a flat plate at various tunnel stagnation temperatures. $M_\infty = 0.85$.

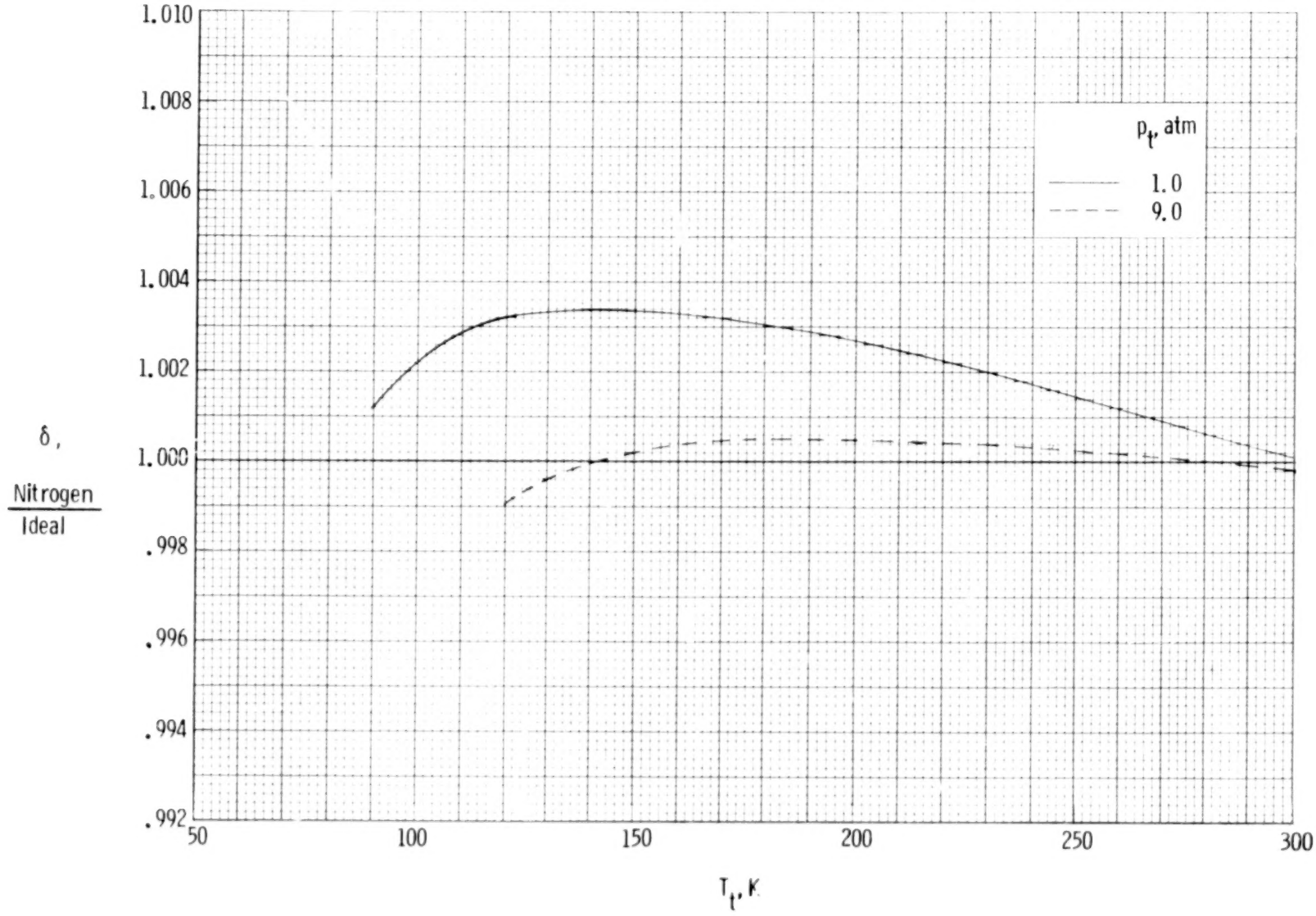

Figure 16.- Relative thicknesses for adiabatic turbulent boundary layers on a flat plate at various tunnel stagnation temperatures. $M_\infty = 0.35$.

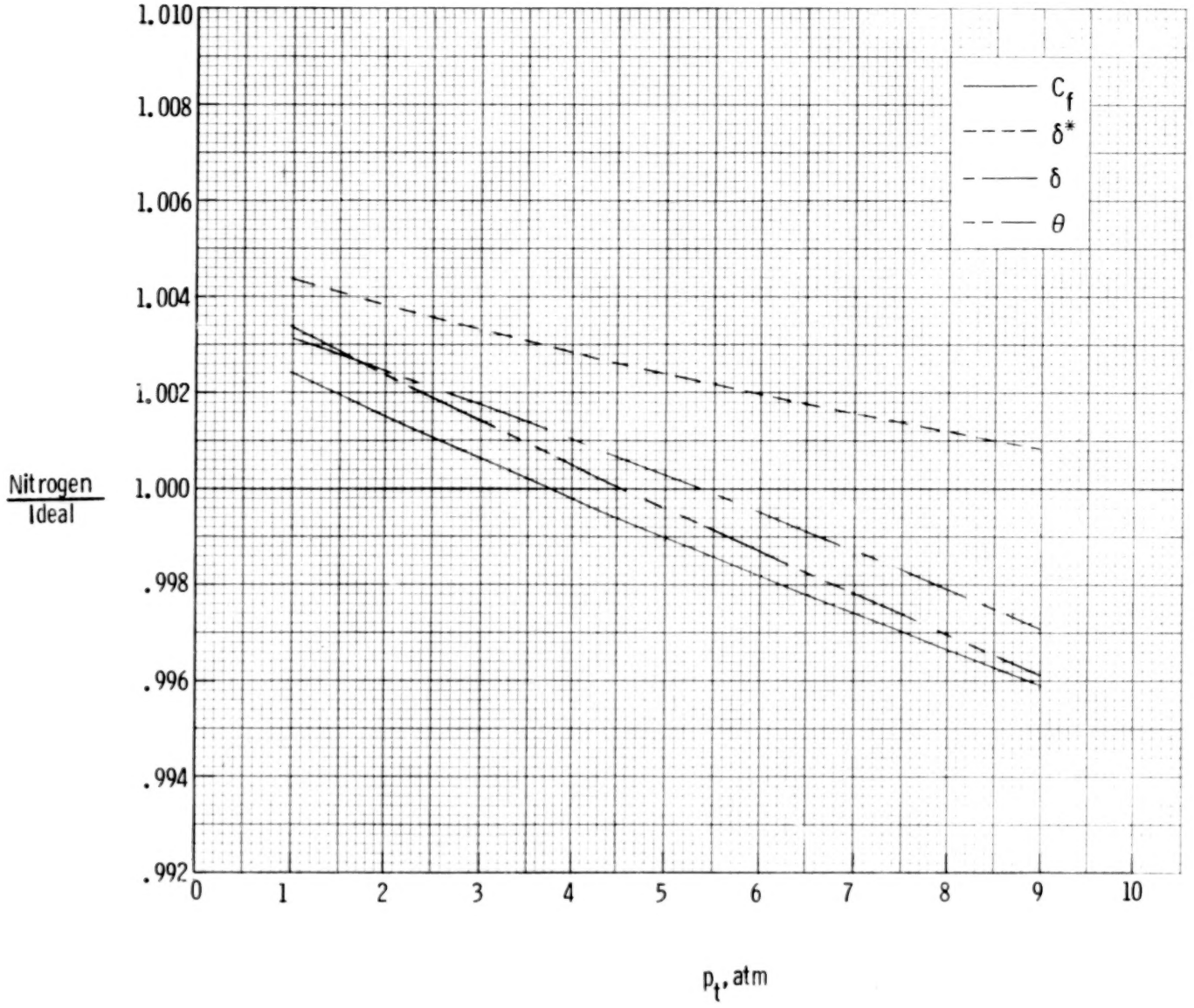

Figure 17.- Relative values for parameters for adiabatic turbulent boundary layers on a flat plate at various tunnel stagnation pressures. $M_\infty = 0.85$; $T_t = 120$ K.

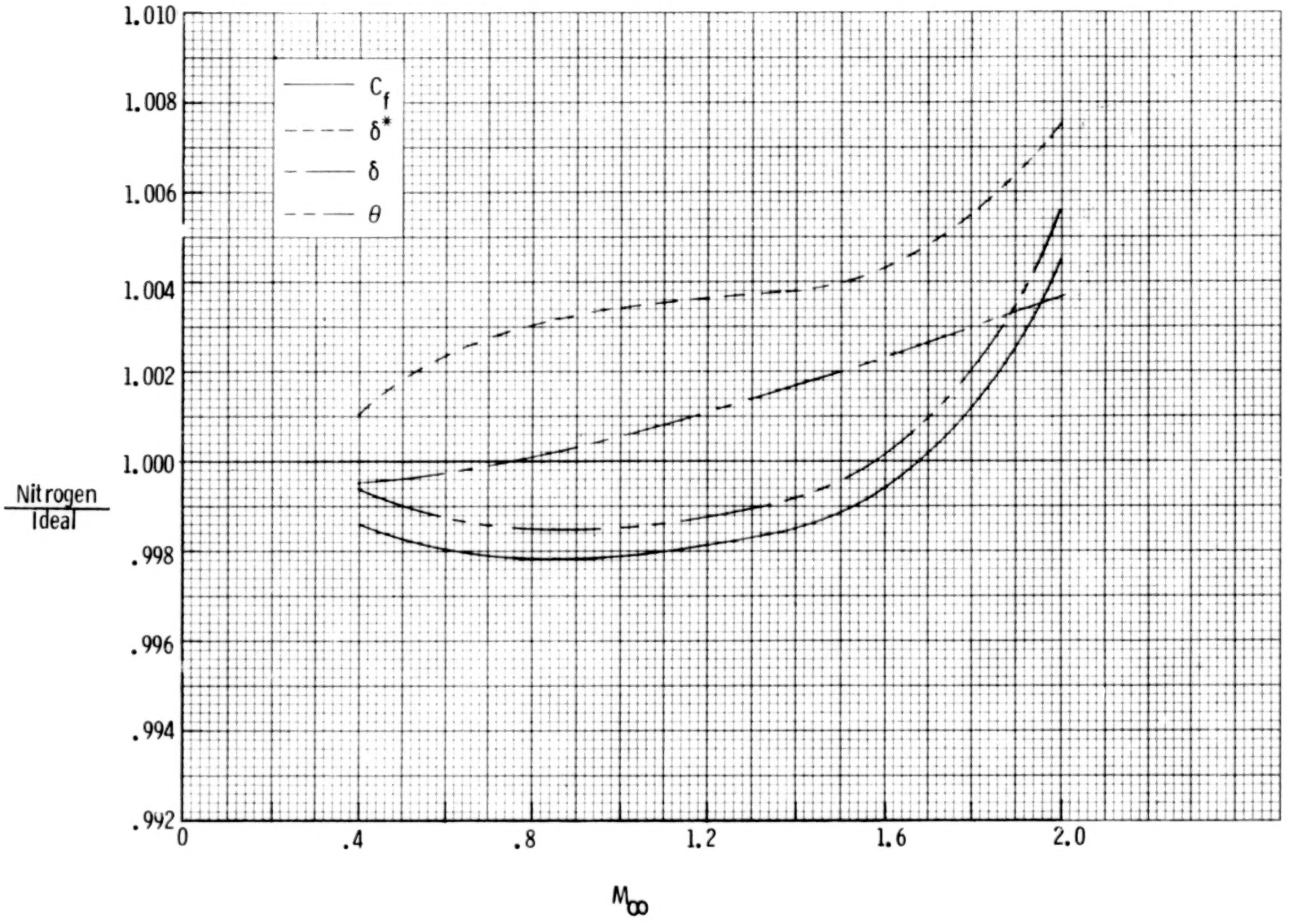

Figure 18.- Relative values for parameters for adiabatic turbulent boundary layers on a flat plate at various free-stream Mach numbers. p_t = 9.0 atm; T_t = 150 K.

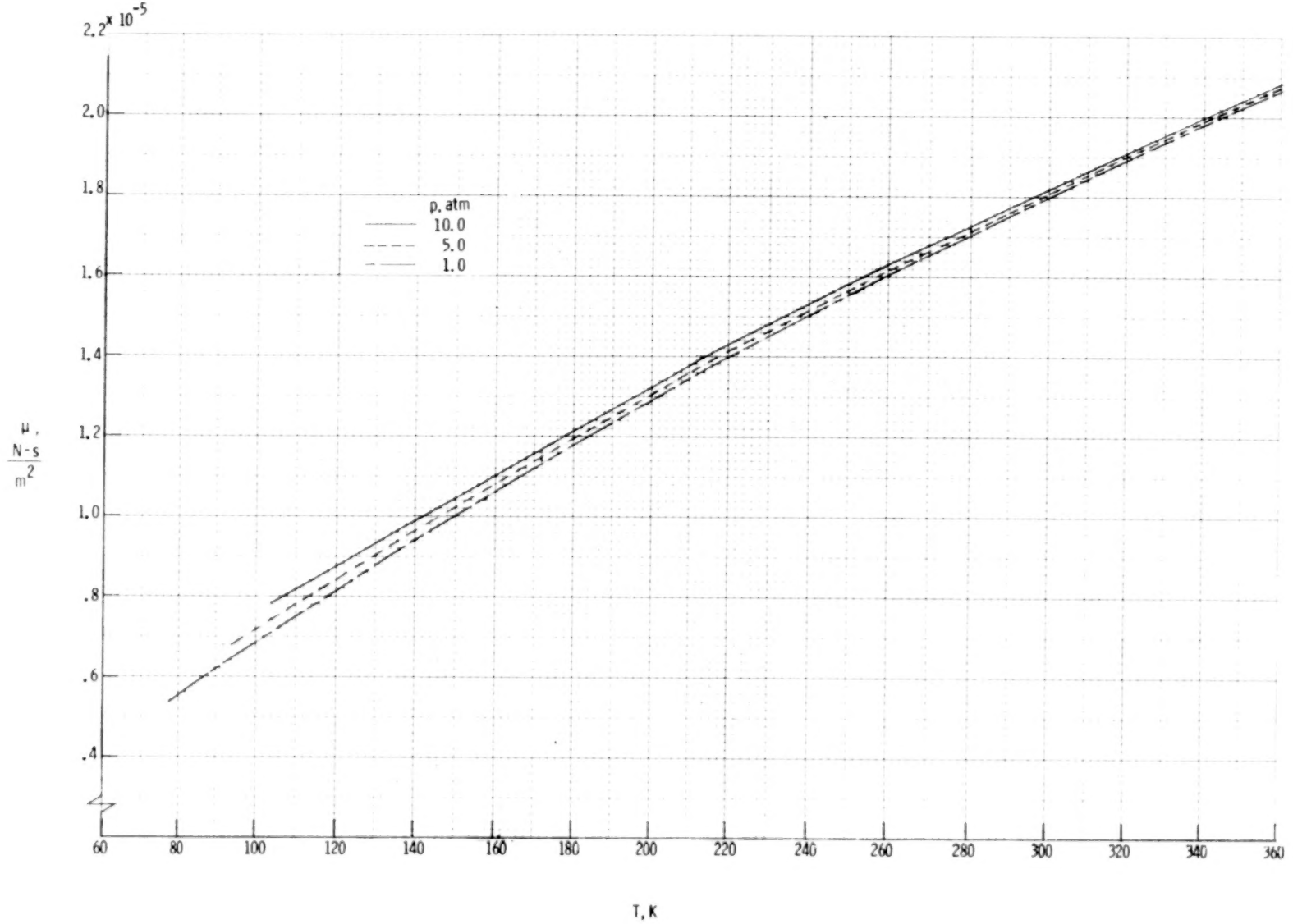

Figure 19.- Viscosity of nitrogen. (Ref. 11.)

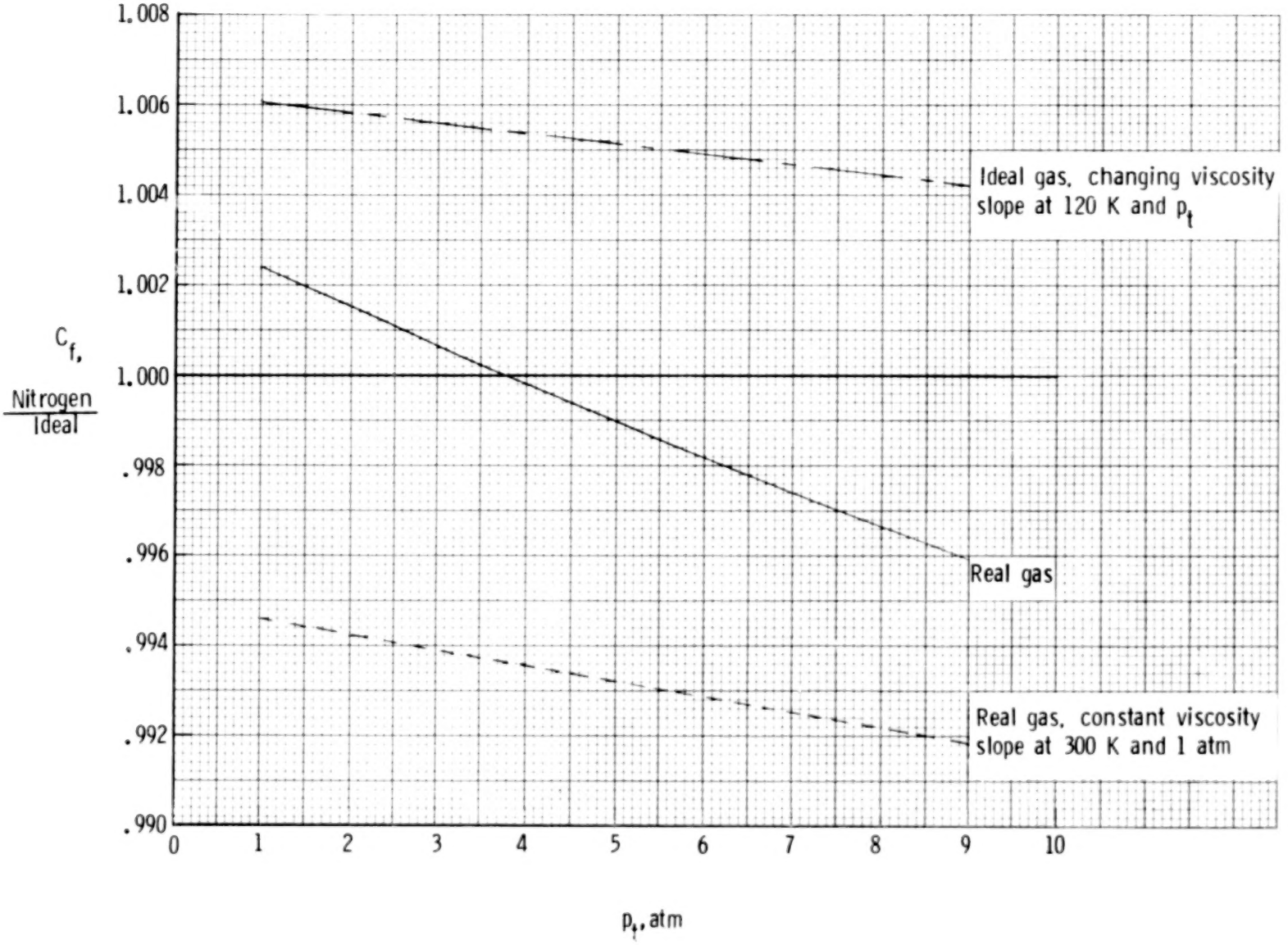

Figure 20.- Relative local skin-friction coefficients for adiabatic turbulent boundary layers on a flat plate according to various solution procedures. $M_\infty = 0.85$; $T_t = 120$ K.

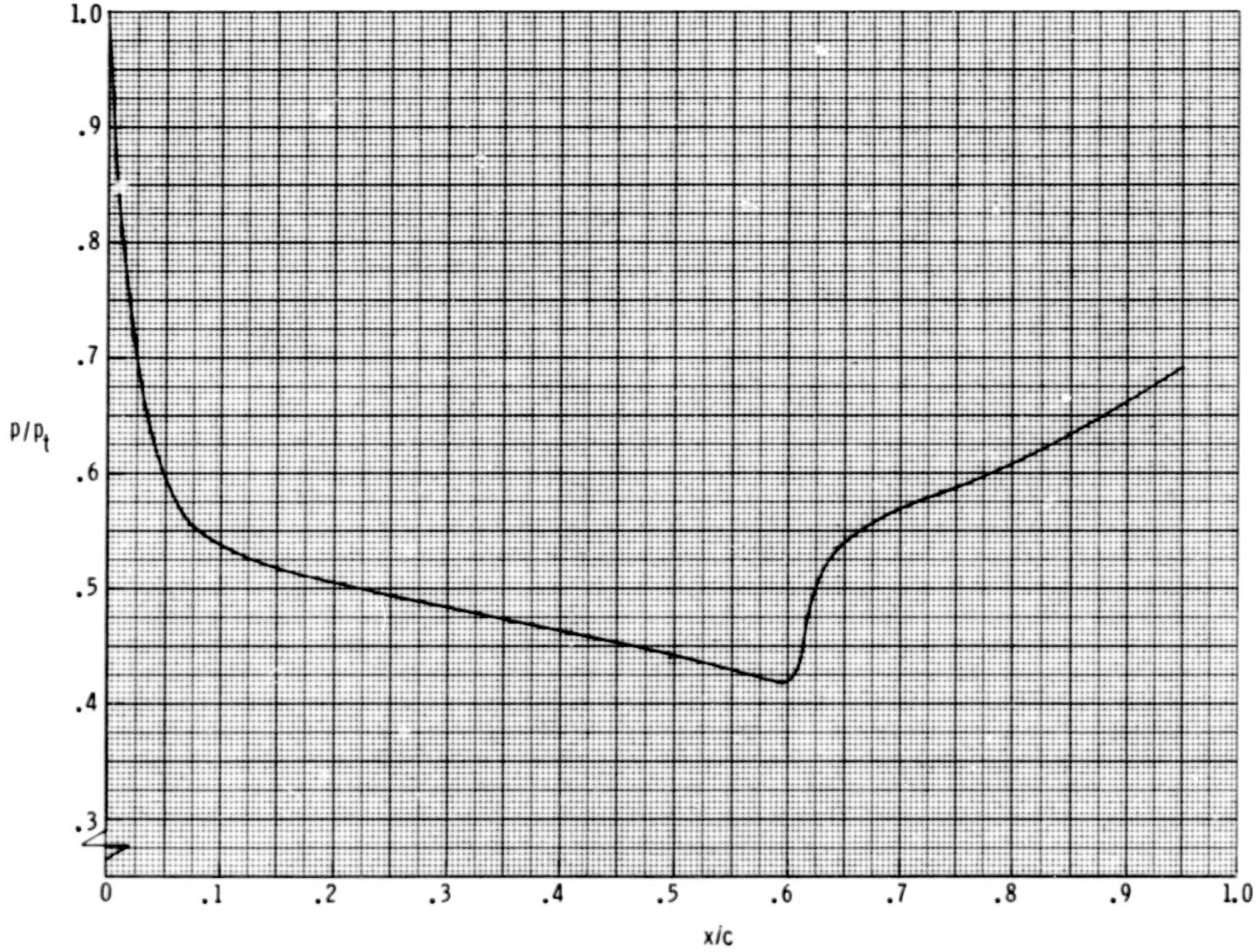

Figure 21.- Pressure distribution for NACA 0012-64 airfoil (ref. 12). $M_\infty = 0.85$; $\alpha = 0^\circ$.

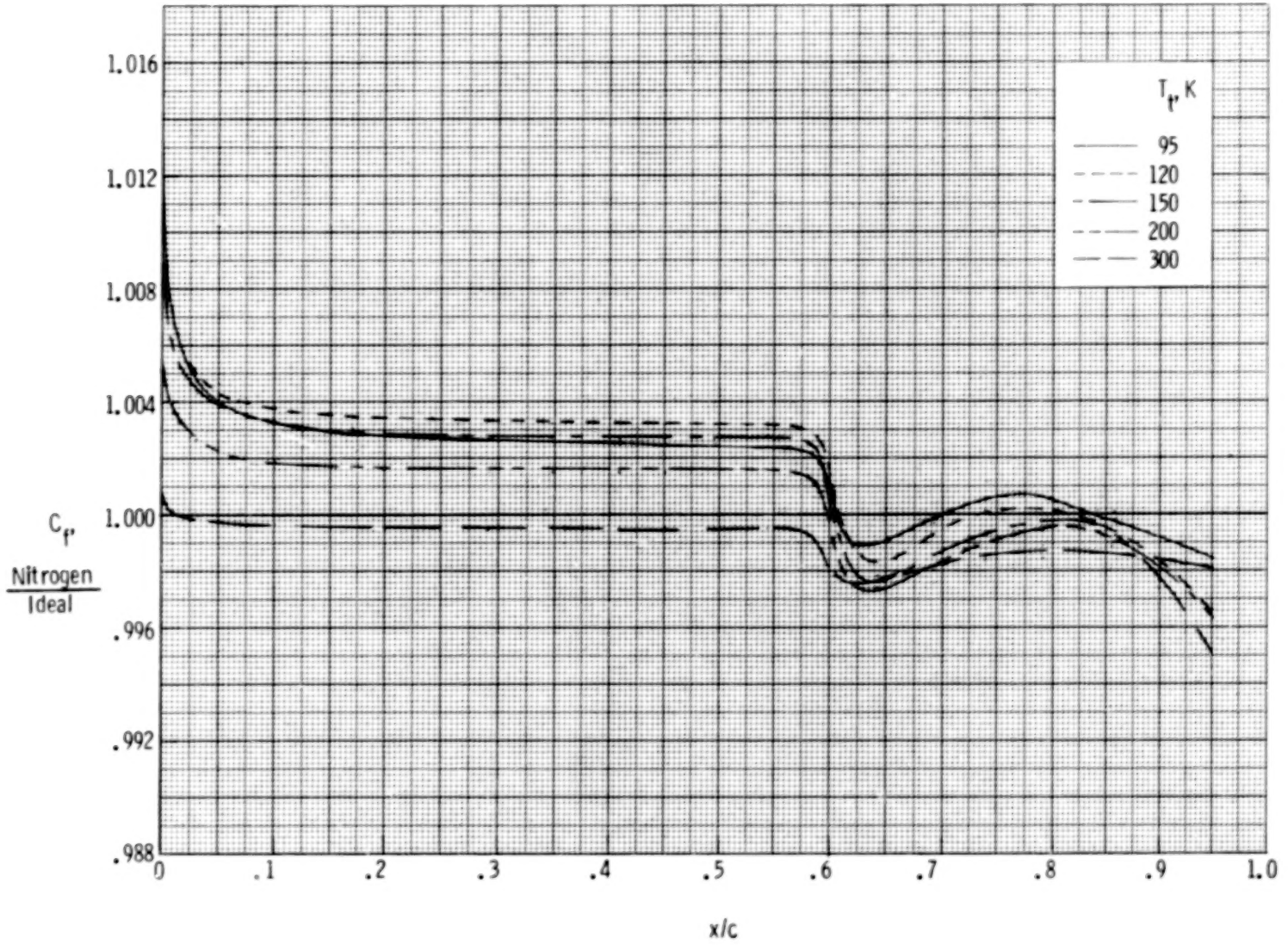

Figure 22.- Relative local skin-friction coefficients for adiabatic turbulent boundary layers on a two-dimensional airfoil at various stagnation temperatures. $M_\infty = 0.85$; $p_t = 1.0$ atm.

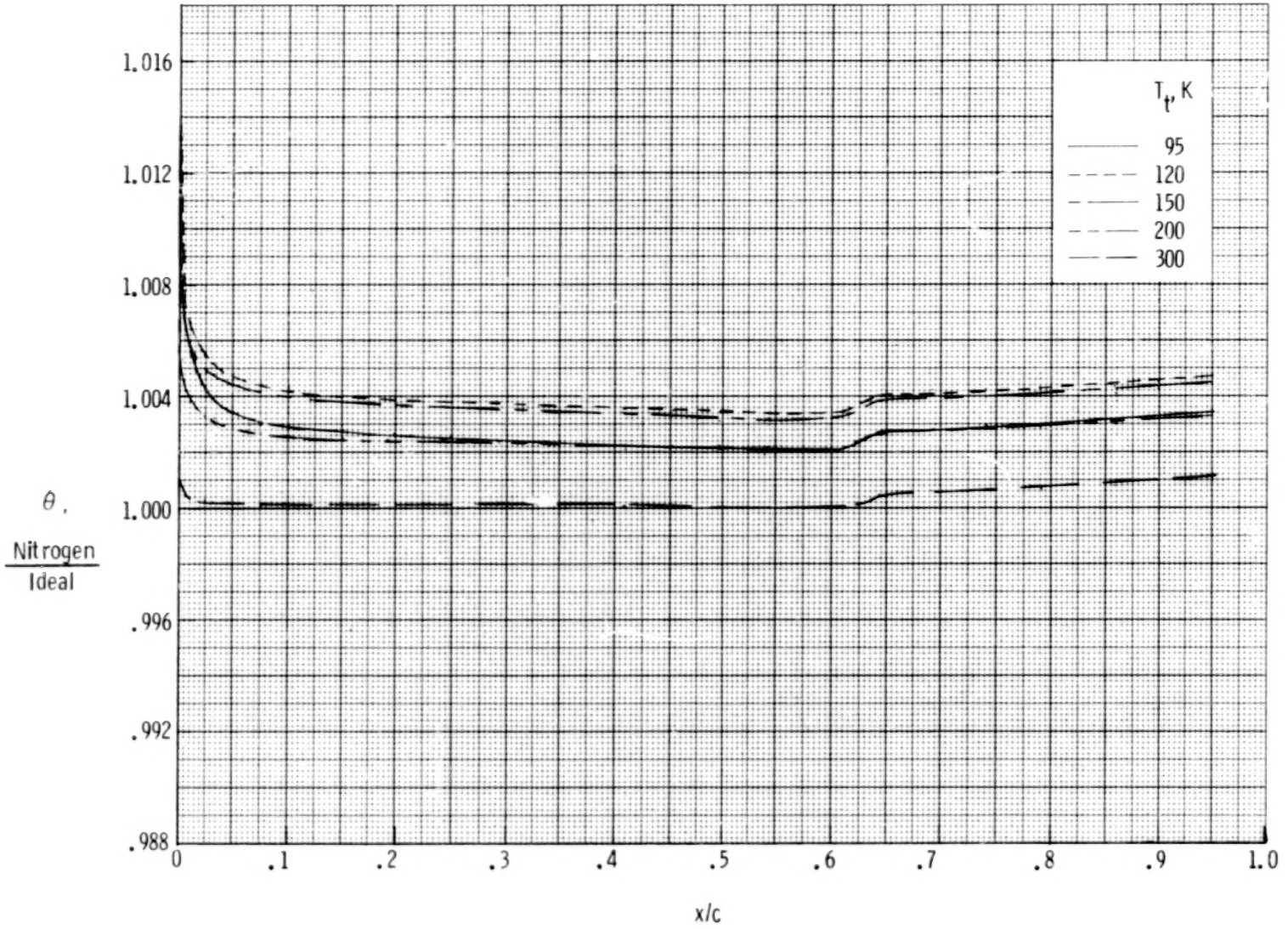

Figure 23.- Relative momentum thicknesses for adiabatic turbulent boundary layers on a two-dimensional airfoil at various stagnation temperatures. $M_\infty = 0.85$; $p_t = 1.0$ atm.

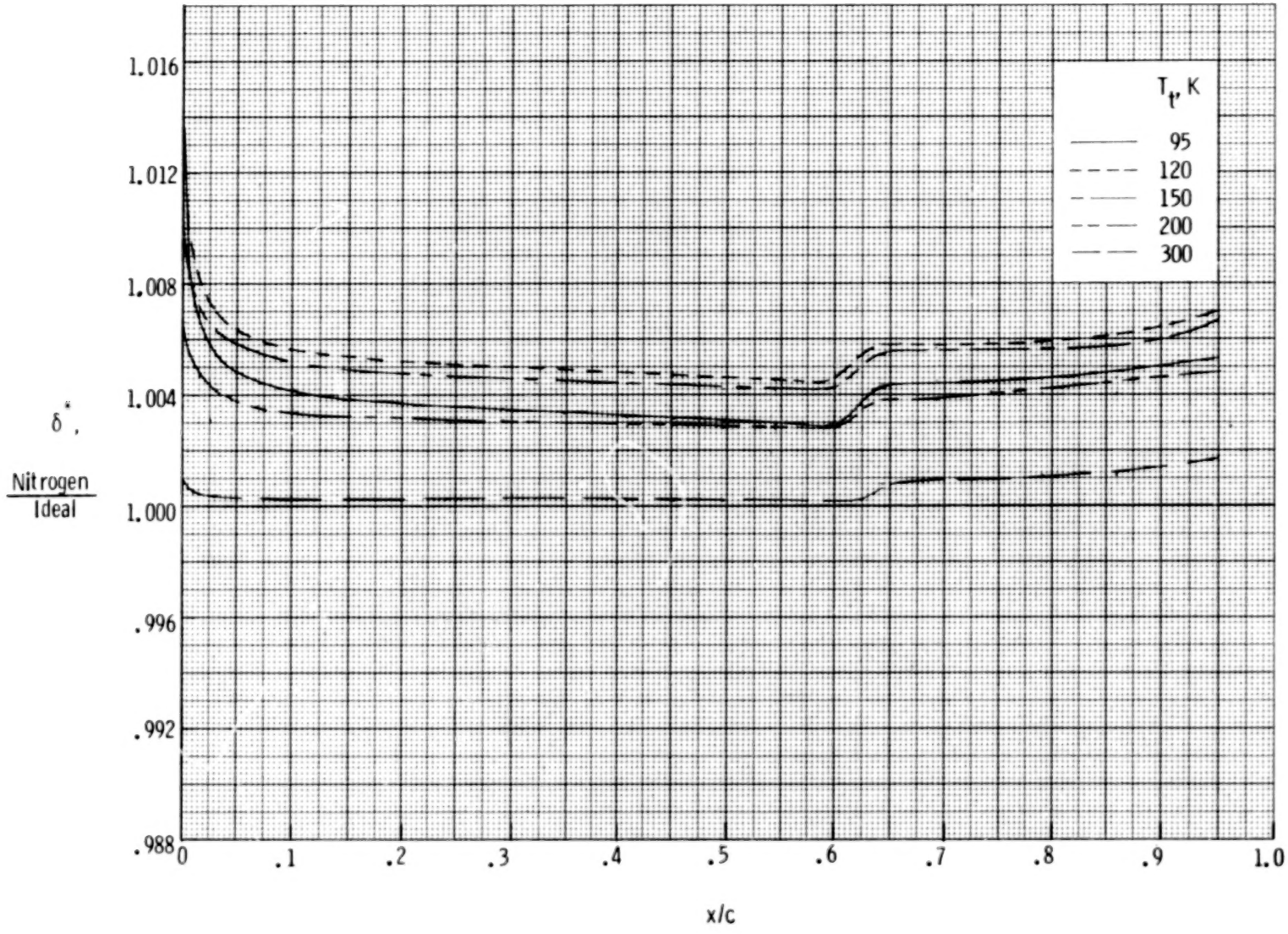

Figure 24.- Relative displacement thicknesses for adiabatic turbulent boundary layers on a two-dimensional airfoil at various stagnation temperatures. $M_\infty = 0.85$; $p_t = 1.0$ atm.

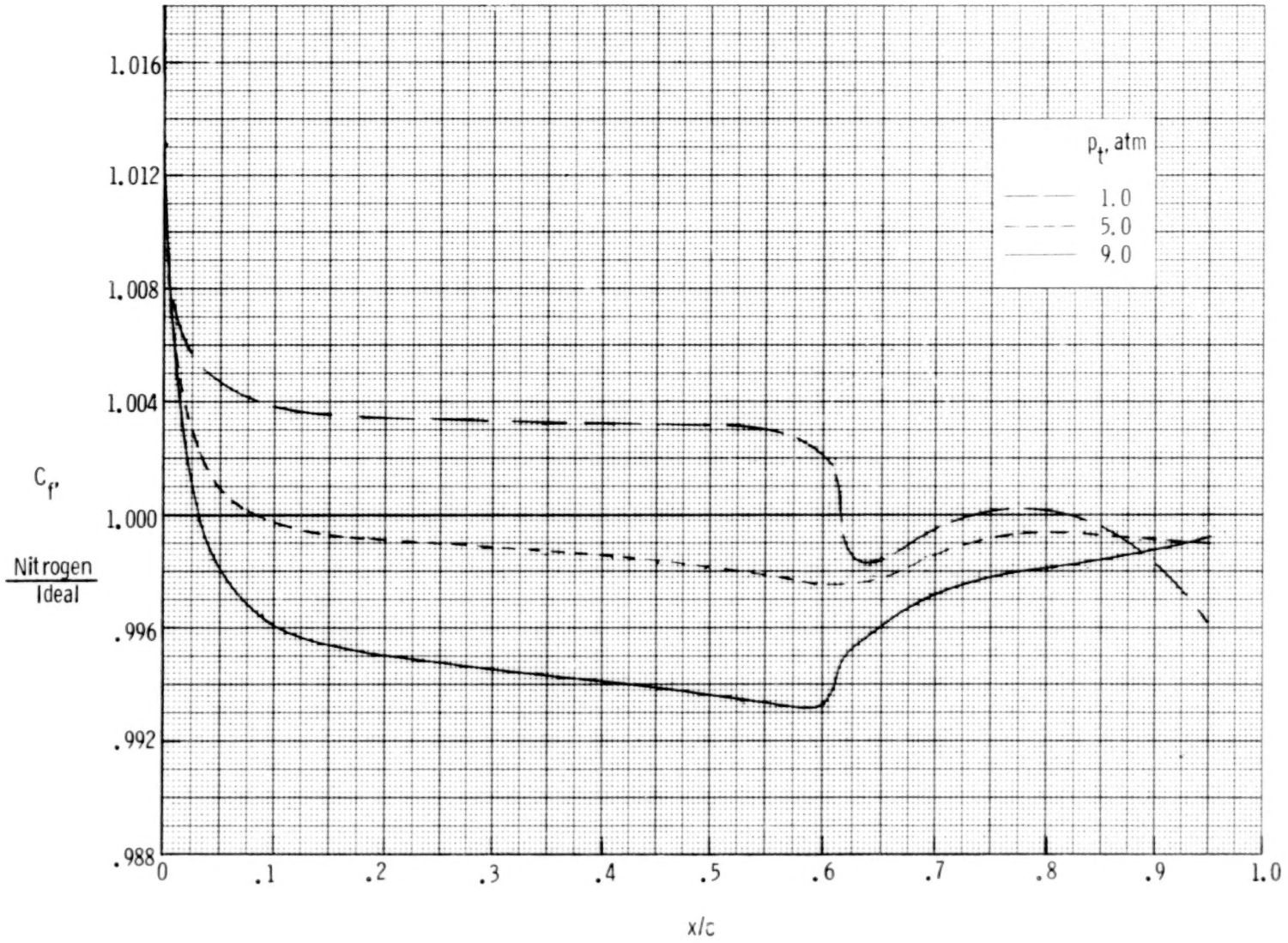

Figure 25.- Relative local skin-friction coefficients for adiabatic turbulent boundary layers on a two-dimensional airfoil at various stagnation pressures. $M_\infty = 0.85$; $T_t = 120$ K.

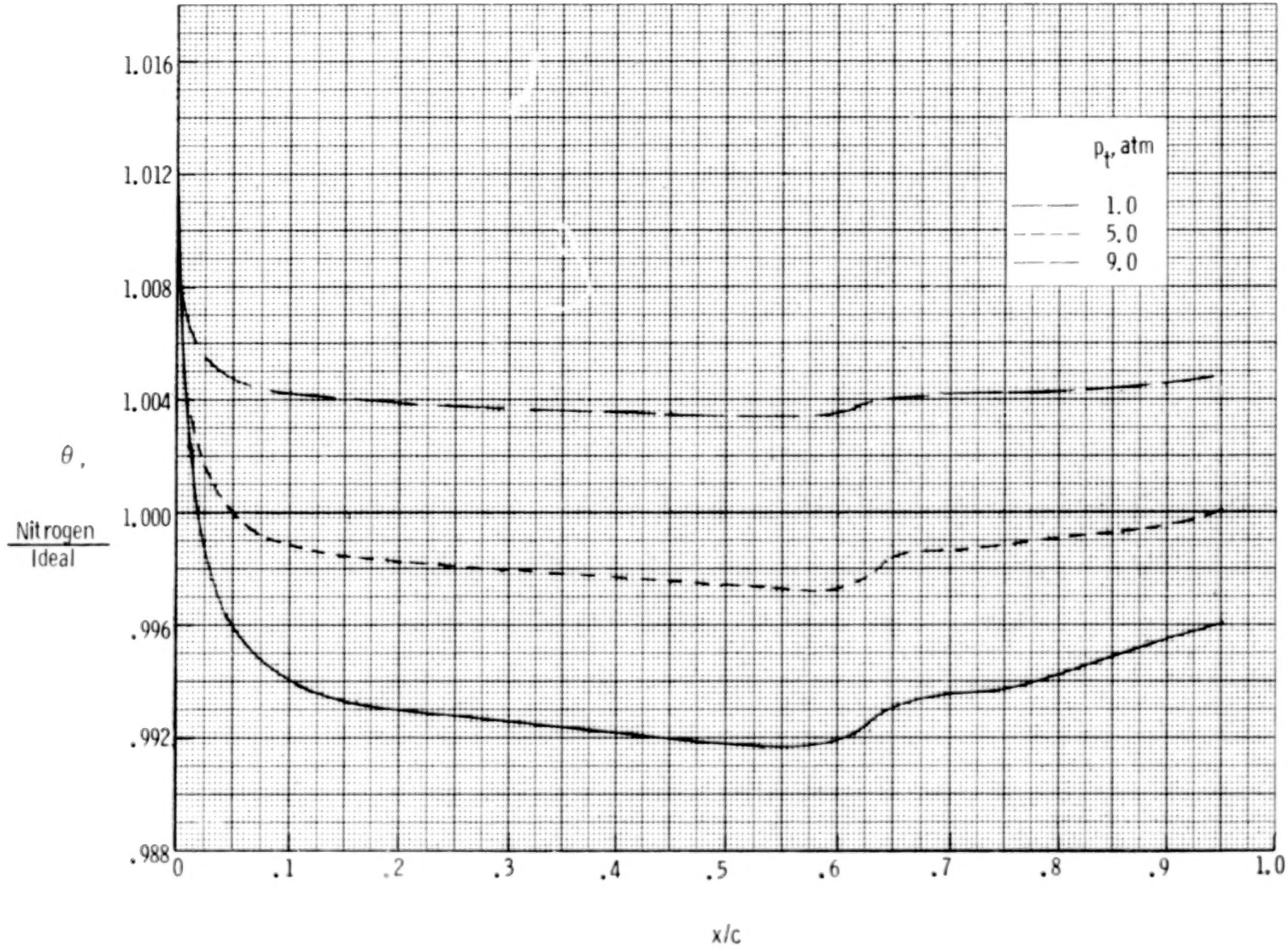

Figure 26.- Relative momentum thicknesses for adiabatic turbulent boundary layers on a two-dimensional airfoil at various stagnation pressures. $M_\infty = 0.85$; $T_t = 120$ K.

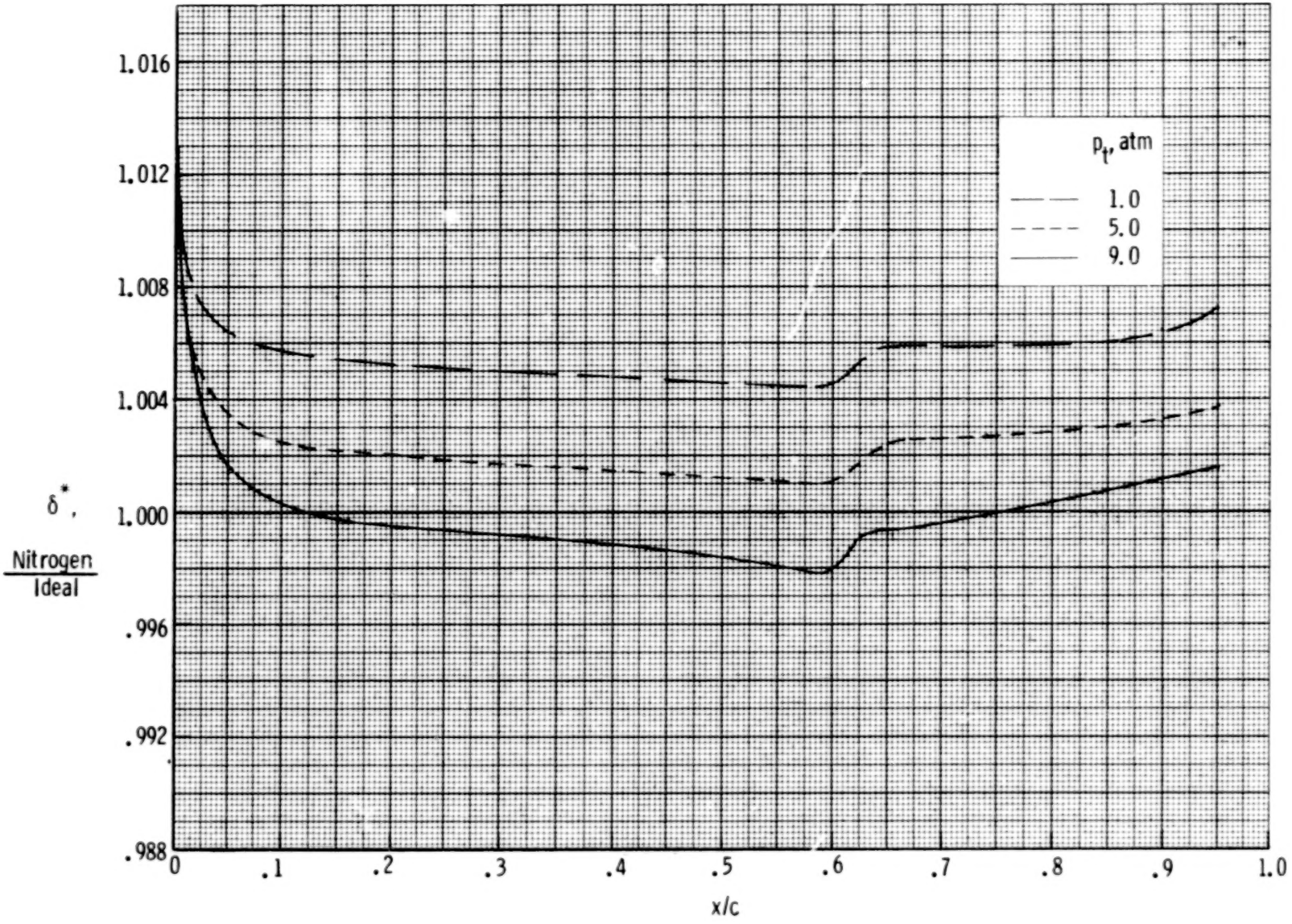

Figure 27.- Relative displacement thicknesses for adiabatic turbulent boundary layers on a two-dimensional airfoil at various stagnation pressures. $M_\infty = 0.85$; $T_t = 120$ K.

1. Report No.	2. Government Accession No.	3. Recipient's Catalog No.
NASA TP-1631		

4. Title and Subtitle	5. Report Date
A THEORETICAL ANALYSIS OF SIMULATED TRANSONIC BOUNDARY LAYERS IN CRYOGENIC-NITROGEN WIND TUNNELS	March 1980
	6. Performing Organization Code

7. Author(s)	8. Performing Organization Report No.
Jerry B. Adcock and Charles B. Johnson	L-13364
	10. Work Unit No. 505-31-53-01
9. Performing Organization Name and Address NASA Langley Research Center Hampton, VA 23665	11. Contract or Grant No.
	13. Type of Report and Period Covered Technical Paper
12. Sponsoring Agency Name and Address National Aeronautics and Space Administration Washington, DC 20546	14. Sponsoring Agency Code

15. Supplementary Notes

16. Abstract

A theoretical analysis has been made to determine the real-gas effects on simulation of transonic boundary layers in wind tunnels with cryogenic nitrogen as the test gas. The analysis included laminar and turbulent flat-plate boundary layers and turbulent boundary layers on a two-dimensional airfoil. The results indicate that boundary layers in such wind tunnels should not be substantially different from ideal-gas boundary layers at standard conditions. At a pressure of 9.0 atm, two separate effects produce deviations of real-gas values from ideal-gas values which are in the opposite direction from deviations at 1.0 atm and are of the same insignificant order of magnitude. Results also show that nonadiabatic boundary layers should be adequately simulated if the enthalpy ratio is the correlating parameter rather than the temperature ratio.

17. Key Words (Suggested by Author(s))	18. Distribution Statement
Wind tunnels Cryogenic Nitrogen Boundary layers	Unclassified - Unlimited Subject Category 09

19. Security Classif. (of this report)	20. Security Classif. (of this page)	21. No. of Pages	22. Price*
Unclassified	Unclassified	37	$4.50

* For sale by the National Technical Information Service, Springfield, Virginia 22161

NASA-Langley, 1980

90 %

50 %